A Feedback Guidance Law for Multi-Revolution Planetocentric Orbital Maneuvering of Solar Sail Spacecraft by Lyapunov Methods

by

Mingde Yin

Supervisor: Christopher J. Damaren

April 2024

B.A.Sc. Thesis

Division of Engineering Science
UNIVERSITY OF TORONTO

The cosmos is all that is or ever was or ever will be. Our contemplations of the cosmos stir us. There is a tingling in the spine, a catch in the voice, a faint sensation: as if a distant memory of falling from a great height. We know we are approaching the grandest of mysteries.

Carl Sagan, *Cosmos*

Abstract

This thesis develops a guidance law for multi-revolution planetocentric maneuvering of a solar sail spacecraft. QUAIL (Q-Law Using Angle of Incidence Limits) adapts the highly successful Q-Law from conventional low-thrust guidance. The first stage uses a Q-Law formulated in modified equinoctial orbital elements which is agnostic of solar sail dynamics, producing an "ideal" thrust direction which is then altered by a heuristic-based second stage to restrict the angle of thrust relative to incident light. Although tampering with the solution produced by the Q-Law relaxes the Lyapunov stability of the guidance law, doing so overcomes the challenge of direction-limited thrust availability inherent to solar sail spacecraft flying planetocentric trajectories; sacrificing instantaneous progress towards the target orbit allows the spacecraft to "wait" until the Sun is in a better position to perform maneuvers requiring particular thrust directions. QUAIL is tested in simulations on a set of complex orbit-to-orbit transfers, achieving convergence in all cases. An extended study to optimize time of flight is performed using stochastic global optimization of guidance parameters, reducing time of flight up to 30%. A further set of cases including $J2$ perturbation demonstrates the robustness of QUAIL against environmental disturbances. Additionally, artificial restriction of the maximum cone angle (for mimicking a real solar sail) is tested, with convergence still achieved under a maximum cone angle of 40°. Overall, the robustness of the underlying Q-Law and the minimal dependence on sail characteristics make QUAIL suitable for developing new solar sail dynamics and mission designs.

Acknowledgements

I have been incredibly fortunate to work with and learn from a multitude of extraordinarily brilliant minds throughout the richest five years of my life. I would like to thank my supervisor, Professor Christopher Damaren for giving me the opportunity to study this topic and for showing me the awe and beauty of spaceflight. I would like to thank Sanjeev for writing the paper that introduced me to the Q-Law and served as the starting point for my understanding of low-thrust spacecraft guidance. I would like to thank my classmates in the Engineering Science program, particularly in the 2T3 Aerospace Engineering cohort for showing me what it means to reach the stars, and for continuously inspiring me to do better. I give particular thanks for Eric, Daniel, Theo, and Rassam for constituting the best capstone teams I could have ever asked for, and for providing the psycho-sociological support I needed to make it here. I would like to thank my course instructors, who, since my first day of EngSci have shaped me into the student I am today. I would also like to thank my high school friends who have kept in touch throughout all these years for sharing with me the rich and enjoyable experiences which have kept me going throughout my undergraduate studies. I would like to thank my parents Xinguo and Yanlu for believing in my dreams of becoming an aerospace engineer, and for all the numerous sacrifices they have undertaken throughout the past twenty three years to afford me the opportunity of realizing my dreams. I would like to thank my sister Connie for showing me a reflection of my own life through growing up, as well as the rest of my family for their encouragements from half a world away.

Contents

List of Figures

List of Tables

Chapter 1

Introduction

PRELIMINARY context for the project is provided, and the main problem is framed around key challenges associated with maneuvering solar sail spacecraft in planetocentric orbits.

1.1 Scope

This project aims to develop a guidance law for performing planetocentric orbital transfers with a solar sail spacecraft, using a simplified feedback approach derived from Lyapunov control theory.

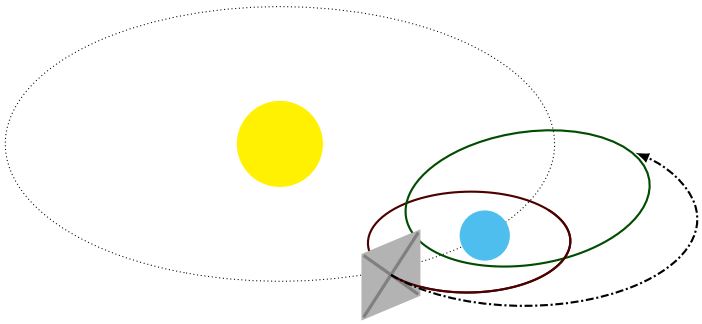

Figure 1.1: Illustratory diagram depicting the main goal of the guidance law.

The goal of the guidance law is to achieve a trajectory solution for a transfer between two orbits around Earth while requiring a minimal set of considerations for the solar sail.

Convergence characteristics and time optimality of the guidance law are considered but are not rigorously assessed or proven. Instead, these characteristics are assessed through

simulations spanning a variety of initial/target orbits and spacecraft configurations.

Three extended studies are performed to investigate the extensibility of the guidance law:

1. Tuning the parameters of the guidance law for minimum time-of-flight;
2. Subjecting the guidance law to disturbances;
3. Testing the guidance law with a more realistic solar sail model.

1.2 Motivation

Low-thrust spacecraft have been the focus of spacecraft guidance research in recent decades, paving the way for the dominance of low-thrust trajectories in contemporary space missions. Electric propulsion has attained widespread adoption [1, 2], while solar sails have remained obscure [3]. Developing practical solar sailing guidance laws is a critical precursor for the acceptance of solar sails as a useful propulsion method.

Earth orbit remains the most prolific destination for space missions, and there exist many proposed applications of solar sailing in this domain. Existing literature is largely focused on specific problems, including orbit raising [4], Earth escape [5], and end-of-life deorbiting [6]. A more general problem of maneuvering solar sail spacecraft between two arbitrary orbits around a planet is considered for this project, as it has received limited study.

1.3 Key Challenges and Gap

Planetocentric orbital maneuvering of solar sail spacecraft poses two significant challenges compared to conventional spacecraft.

1. Solar sails produce little thrust [7], making classical impulse-based orbital maneuvering theory unsuitable for trajectory planning. Low-thrust trajectory planning for planetocentric orbits is itself a challenging domain of study; traditional approaches using global trajectory optimization struggle with the "winding" nature of consecutive orbits.
2. Thrust is dependent on the orientation of the spacecraft relative to incoming sunlight. Thrust availability depends on the direction of incident light, which cannot be directly controlled. For example, a solar sail cannot produce thrust directly towards incoming sunlight, akin to a sailboat sailing directly into the wind. Furthermore, real solar

sails are typically limited in terms of how much they can be misaligned from incident sunlight, owing to both thrust production and attitude control needs [7].

Low-thrust planetocentric orbital maneuvering has been approached using methods derived from feedback control theory [8–11]. Instead of approaching trajectory guidance as a global optimization problem, feedback guidance laws trade global optimality for better convergence behaviour and simplicity. This class of guidance laws has been explored in the context of solar sailing but formulated with an assumed form of relationship between sail thrust and orientation relative to the Sun. Notably, a recent guidance law developed by Oguri (2023) [12] depends on 3 parameters representing the contributions of different modes of light reflection.

A key appeal of feedback guidance laws is their relative independence from system parameters. It is therefore appealing to consider a solar sailing guidance law that agnostic to the parameters of the solar sail. Such a guidance law would facilitate trajectory analysis for unique and esoteric spacecraft designs, and remain applicable as better reflectivity models for solar sails are developed.

1.4 Implementation

The guidance law is implemented as a two-stage algorithm, combining a solution obtained from conventional low-thrust feedback guidance theory with an additional set of adaptations to make the solution amenable to solar sails.

The first stage is based on a control-Lyapunov function, Q, in a formulation called the *Q-Law* first introduced by Petroupolos (2004) [9]. A reformulation presented by Varga and Pérez (2016) [10] using analytical approximations to the derivatives of Q is used to produce a desired sail orientation based on a spacecraft state in modified equinoctial orbital elements. The intermediate guidance solution is then adapted to obey constraints associated with the alignment of the sail relative to incoming sunlight.

A computer model of the guidance law is tested in simulations. A MATLAB implementation is used for high-fidelity simulations and performance validation. A lower-fidelity but faster implementation in C is used to optimize the parameters of the guidance law for minimum time-of-flight. Extended studies for perturbations and realistic solar sail models are implemented in the MATLAB codebase.

Chapter 2

Background

An in-depth discussion of the background associated with the project is presented, discussing specific topics driving the approach taken to solving the problem. The literature review is divided into four sections:

1. Spacecraft trajectory guidance at large, for which solar sail guidance is a subset;
2. Feedback guidance laws, particularly the Q-Law derived from Lyapunov control theory;
3. Special considerations needed for solar sails beyond conventional low-thrust spacecraft;
4. Approaches to solar sail guidance, particularly planetocentric orbital maneuvering.

2.1 Spacecraft Trajectory Guidance at Large

This section covers essential aspects of spacecraft orbits, followed by a discussion of various approaches used to develop guidance laws for orbital maneuvering. Techniques for low-thrust spacecraft are given focus, as those are most relevant to solar sails.

2.1.1 The Planetocentric Guidance Problem

The general problem of planetocentric orbital maneuvering refers to altering the orbit of a spacecraft around a parent celestial body from some initial orbit to a final target orbit. (Note that this is different from *rendezvous*, which adds a further constraint that the spacecraft must reach a certain point along the target orbit at a specific time, i.e. to meet with a spacecraft already in that target orbit.)

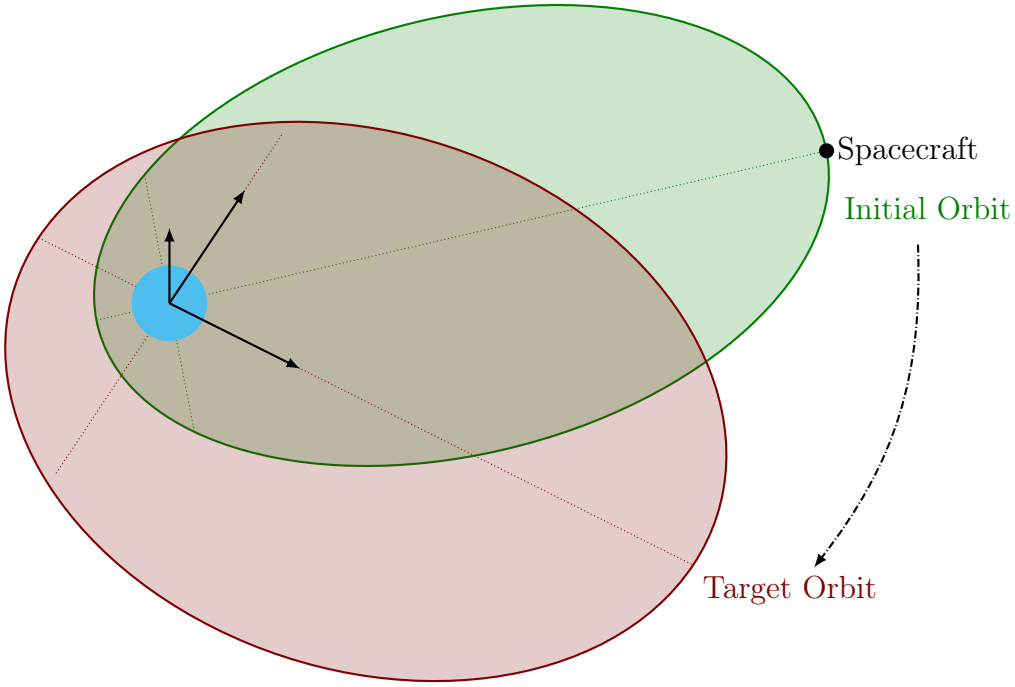

Figure 2.1: Cartoon illustration of the planetocentric orbital maneuvering guidance problem.

Solving the guidance problem refers to generating a sequence of applied thrust vectors that modify the spacecraft's orbit accordingly. Since the solution is generally not unique, the space of all valid guidance solutions can be searched for those that result in the shortest time of flight or the least propellant expenditure, for example. Hence, the guidance problem is often considered approached as an optimization problem [13].

2.1.2 Description and Evolution of Spacecraft Orbits

Orbits (in the context of the two-body problem) are described using a set of 6 orbital elements [14]. Keplerian orbital elements are the most prolific, but there exist alternative formulations of two-body spacecraft orbits which also result in 5 elements specifying orbital geometry/orientation and 1 element representing time.

Some examples:

- Keplerian Elements $\{a, e, i, \Omega, \omega, \theta\}$
- Modified Equinoctial Elements $\{p, f, g, h, k, L\}$ [15]
- Gooding Universal Elements $\{\alpha, q, i, \Omega, \omega, \tau\}$ [16]

Altering the orbit of a spacecraft to solve the guidance problem involves changing its orbital elements. The process of solving for the evolution of orbital elements in time is known as *orbit propagation*.

Cowell's method [14] is a well-known way of propagating general spacecraft trajectories in Cartesian state space. Typically this involves integrating equations of motion derived from Newton's second law in a form similar to the following:

$$\frac{\mathrm{d}^2}{\mathrm{d}t^2}\boldsymbol{r} = -\frac{\mu}{||\boldsymbol{r}||^3}\boldsymbol{r} + \boldsymbol{f}_\mathrm{p} \tag{2.1}$$

Wherein $\boldsymbol{f}_\mathrm{p}$ is some perturbing acceleration (i.e. unrelated to point-mass gravity of the central body) and $\boldsymbol{r}$ is the position vector of the spacecraft (both expressed in an inertial frame). Although simple at first glance, a difficulty of working in Cartesian coordinates for spacecraft guidance is that all six values of the state vector (position and velocity) change in time, regardless of the presence of perturbations. Additionally, describing the geometry of an orbit in terms of a Cartesian state is not as straightforward as using orbital elements.

Variational Methods for Orbit Propagation

Variational equations of motion are ordinary differential equations giving the time derivatives of orbital elements when subject to a perturbing acceleration, such as thrust from a propulsion system. Taking Keplerian elements as an example, they take the form:

$$\frac{\mathrm{d}}{\mathrm{d}t}\begin{bmatrix} a \\ e \\ i \\ \Omega \\ \omega \\ \theta \end{bmatrix} = A\boldsymbol{f}_\mathrm{p} + \boldsymbol{b}$$

Where $A \in \mathbb{R}^{6\times 6}$, $\boldsymbol{b} \in \mathbb{R}^6$, and typically only the last entry of $\boldsymbol{b}$ is nonzero (i.e. the other 5 orbital elements are invariant when there is zero perturbing acceleration).

When posed in terms of variational equations of motion, the guidance problem becomes one of determining the perturbing acceleration needed at each instant in time to **change the orbital elements of the spacecraft which describe the geometry and orientation of the orbit** (e.g. in the case of Keplerian elements, a, e, i, Ω, ω).

Compared to Cowell's method, working directly in orbital elements dramatically simplifies the analysis of guidance laws, particularly in discussing convergence to the target orbit.

Comparison with Classical Orbital Maneuvering Theory

Classical orbital maneuvering theory employs brief, high-thrust maneuvers that are approximated as impulses, leading to a sequence of discrete orbits constituting a maneuver, and removing the need to analyze trajectories in terms of continuous equations of motion. Impulse-based maneuvering theory has been extensively studied and is commonly taught at the undergraduate level, as demonstrated by books such as Ref. [14]. On the other hand, low-thrust guidance requires time integration of differential equations, making the majority of analysis **heavily reliant on numerical simulation**. One common approach used for solving the guidance problem for a (low-thrust) solar sail spacecraft is to **integrate the variational equations of motion**.

2.1.3 The Case for Modified Equinoctial Elements

The 5 Keplerian elements describing the geometry and orientation of an orbit are the semi-major axis (a), eccentricity (e), inclination (i), right ascension of the ascending node (Ω), and argument of periapsis (ω). The remaining orbital element used to represent time is the true anomaly (θ). A significant challenge associated with using Keplerian elements and their respective variational equations in trajectory analysis is the occurrence of**singularities** for many types of orbits (e.g. circular orbits, zero-inclination orbits). Although no orbits are perfectly circular or zero-inclination in practice, the singularities appearing in both the orbital elements themselves and their associated variational equations cause numerical issues in simulations.

Common solutions to this include adding "deadbands" to the values of eccentricity and inclination, such when they are decremented under some threshold (e.g. $|e| < 10^{-4}$), their value is clamped to the lower bound until their rates of change become positive. This is the approach taken by Petropoulos (2004) [9] to avoid reaching singularities.

Modified equinoctial orbital elements defined by Walker et. al (1985) [15] remove singularities in all cases except for a perfectly retrograde equatorial orbit, and present many numerical conveniences for analysis. They are defined from Keplerian elements as follows:

$$
\begin{aligned}
p &= a\left(1-e^2\right) & h &= \tan(i/2)\cos\Omega \\
f &= e\cos(\omega+\Omega) & k &= \tan(i/2)\sin\Omega \\
g &= e\sin(\omega+\Omega) & L &= \Omega+\omega+\theta
\end{aligned}
$$

In contrast to Keplerian elements, the modified equinoctial elements (f, g, h, k) describing the orientation of the orbit represent ratios instead of angles, and are order unity (when

$i \in [-90° \, 90°]$). Perfectly circular and equatorial orbits are handled without issues in the variational equations of motion (shown later in Equation 3.3).

The heavy dependence of numerical simulation for the analysis of low-thrust spacecraft trajectories makes modified equinoctial elements a good basis for developing a guidance law.

2.1.4 Global Optimization Methods for Low-Thrust Trajectories

One common approach used for low-thrust trajectory planning is posing the guidance problem as a global optimization problem. At a high level, there exist two main classes of methods: direct and indirect methods, along with variants thereof. These are presented in depth in a survey of the state of the art by Morante et al. (2021) [17], but the essential points are discussed here. Note that global methods often employ a Cartesian state formulation instead of orbital elements.

Both methods construct a sequence (i.e. a time history) of control inputs that bring the spacecraft to a targeted state. Both methods also discretize the problem by assuming a certain form for the control inputs (e.g. piecewise polynomials). Direct methods solve for unknown coefficients using pseudospectral or other collocation-based methods through integration of the equations of motion and direct evaluation of the functional to be optimized. Indirect methods (also referred to as adjoint, co-state, or primer vector methods) use variational techniques and Lagrangian multipliers to produce systems of equations with sufficient constraints for optimality which are then solved to get the unknown coefficients. As described by Kelly (2015) in an introductory overview paper of global optimization [18], direct methods find coefficients to minimize a functional, while indirect methods solve a system of equations which "set the gradient of the functional to be zero".

For interplanetary missions, the timescale of the astrodynamics (i.e. the period of orbits around the Sun) is similar to the timescale of the optimization problem (i.e. the time of flight), making the problem computationally tractable through the use of a coarse discretization. The Sims-Flanagan method, a direct method, is highly amenable for interplanetary trajectories [13, 19]. Collocation-based methods (e.g. Gauss pseudospectral methods) are used in similar applications [20, 21].

A critical weakness of global optimization approaches for trajectory planning is their dependence on an initial guess. Indirect methods in particular struggle with stably converging to a solution when presented with a poor initial guess. For simple interplanetary trajectories, intuition is sufficient to kickstart an optimization, but the complex nature of orbital transfers

around a planet is considerably less intuitive.

As discussed in the introduction, a challenging aspect of planetocentric orbital maneuvering is the mismatch in timescales between orbital periods and time of flight. Referred to as **multi-revolution transfers**, trajectories making a large number of revolutions around a planet require basis functions with sufficiently high spatial frequency to accurately capture the "curvature" of the orbits. An extremely low-thrust propulsion system such as a solar sail may need hundreds of revolutions to raise its orbit, requiring either a very high order basis or a large number of basis functions – both of which result in a challenging computational workload.

Consequently, this project focuses on an entirely different approach to spacecraft guidance – locally optimal feedback guidance.

2.2 Feedback Guidance Laws

Classical control theory is built upon the idea of simple feedback control loops. Although designed without any guarantees for global optimality, they are simple to implement and can be tuned to get near-optimal performance.

The same idea has been applied to guidance in two main forms: thrust-blending and Lyapunov control. Both approaches use formulations using orbital elements for state representation. In both cases, the key idea is to take the difference between the current/target value for each orbital element and produce a control input that decreases the error at each timestep. Removing the dependence on modelling a coupled global trajectory dramatically decreases computational complexity, and has the added benefit of being easy to run "online" with simulators in a feedback loop.

Thrust-blending (also referred to as blended control) methods find control inputs that independently maximize the rate of decrease of the error for each of the orbital elements, and take a linear combination of the individual inputs. This is examined more thoroughly in the survey by Morante et al. (2021) [17].

Lyapunov methods can be thought of as a variant of thrust-blending methods, by using a heuristic to weigh the decrease in error for each orbital element by an optimality criterion. The specific linear combination taken is the one that maximizes the rate of decrease of some scalar function, described in the next section.

2.2.1 Lyapunov Methods

A brief primer on Lyapunov control theory is presented, based on an explanation from the fundamental paper of planetocentric Lyapunov-based guidance by Ilgen (1994) [8].

Consider a dynamic system with state $x(t) \in \mathbb{R}^n$ a control input $u \in \mathbb{R}^m$ governed by some differential equation $f : \mathbb{R}^n \times \mathbb{R}^m \to \mathbb{R}^n$ s.t. $\dot{x}(t) = f(x(t), u)$.

Consider a function $V : \mathbb{R}^n \to \mathbb{R}$, called a **potential function or control-Lyapunov function**, which maps each state value to some scalar. Intuitively, this can be thought of as analogous to the potential energy of the system, which vanishes at some point $x = \hat{x}$, e.g. a mass attached to a spring, wherein $V(x) = \frac{1}{2}(x - \hat{x})^2$

This dynamic system is said to be **Lyapunov stable** iff a potential function can be found which meets the following conditions:

1. $V(x) > 0 \; \forall \; x \neq \hat{x}$
2. $V(\hat{x}) = 0$
3. There exists some u for all $x \in \mathbb{R}^n$ s.t.

$$\dot{V} = \nabla V(x) \cdot \dot{x}(t) = \nabla V(x) \cdot f(x, u) < 0$$

where $\nabla V(x)$ means $\dfrac{\mathrm{d}V}{\mathrm{d}x_i} = \left\{ \dfrac{\mathrm{d}V}{\mathrm{d}x_1}, ..., \dfrac{\mathrm{d}V}{\mathrm{d}x_n} \right\}$

Or in other words:

- $V(x)$ is positive definite
- For every state, there exists a control input which decreases $V(x)$ in time.

Over time, this is guaranteed to drive the state towards $x = \hat{x}$, so long as the stabilizing control input is provided.

This is a powerful idea because it can be used both as a means to prove the stability of a system, and also as a means of developing a feedback control law $u = u(x, t)$

Solving for the value of u at each value of x such that $\dot{V}$ is minimized produces a **locally optimal feedback control law**.

By introducing an optimality criterion, a unique solution can be obtained at each timestep. Lyapunov control is hence a natural extension of thrust blending.

2.2.2 Early Control-Lyapunov Functions

Ilgen's paper proposes a potential function which is a linear combination of the square of the difference between each orbital element and its target value. Formulated in Keplerian elements, it is given as:

$$V = \frac{1}{2}\left[P_1\frac{(a-\hat{a})^2}{R_e^2} + P_2(e-\hat{e})^2 + P_3(i-\hat{i})^2 + P_4(\Omega-\hat{\Omega}) + P_5(\omega-\hat{\omega})^2\right] \tag{2.2}$$

where hatted values refer to target orbital elements, and $P_i, i \in \{1, ..., 5\}$ are weighting factors.

At each timestep, the only thing needed to compute the control input is the current state of the spacecraft – there is **no dependence on past or future states**, making the guidance law extremely cheap computationally.

Additionally, given the relatively simple nature of the potential function, it is possible to derive analytical expressions for the control input. However, given that Ilgen's potential function is expressed in Keplerian elements, there are singularities in the derivatives of V.

Nonetheless, Ilgen demonstrates **nearly time-optimal behaviour** from this guidance law, making it a competitive alternative to global methods.

Importantly, Ilgen demonstrates guaranteed convergence to the final target orbit under certain limiting conditions. This is remarkable, as **no knowledge of the global solution is needed** to converge to the target orbit. However, a complete analysis of convergence in the general case is not given.

This paper highlights many of the key strengths and weaknesses of Lyapunov methods for guidance. While Lyapunov methods are simple to implement, cheap to simulate, and performant, it is challenging to rigorously analyze the performance of feedback guidance laws, particularly concerning convergence guarantees and convergence rate. The lack of coupling to the global solution makes it difficult to robustly ascertain that a locally optimal solution can be extended to the global domain.

Another example of a control-Lyapunov guidance law is demonstrated by Naasz [22].

A notable contemporary development in Lyapunov-based planetocentric orbit maneuvering guidance is a family of guidance laws spawned from the Q-Law.

2.2.3 The Q-Law Family

The Q-Law was developed by Petropoulos [9] using a potential function of the form:

$$Q = (1 + W_P P) \sum_{\text{œ}} W_{\text{œ}} S_{\text{œ}} \left(\frac{\text{œ} - \hat{\text{œ}}}{\dot{\text{œ}}_{\max}} \right)^2, \quad \text{œ} \in \{a, e, i, \Omega, \omega\} \tag{2.3}$$

where P is a penalty function used to impose constraints, $S_{\text{œ}}$ is a scaling function for each orbital element, and $W_\sigma, \sigma \in \{P, a, e, i, \Omega, \omega\}$ are weights. $\hat{\text{œ}}$ represents target orbital elements, and $\dot{\text{œ}}_{\max}$ represents the maximum attainable rate of change in each orbital element across the course of an orbit (i.e. across all values of θ) and across all thrust directions (assuming a propulsion system with fixed thrust).

Q is described as a "proximity quotient"; each term in the summation can be thought of as the square of the minimum time needed to drive the error in a single orbital element to zero.

One of the key brilliancies of the approach is implementing a means to compensate for **how "easy" it is to change a given orbital element** (through $\dot{\text{œ}}_{\max}$). Orbital elements that have a lower possible maximum rate of change are weighed with more importance by the potential function. This mechanism allows for the error in each orbital element to "balance out" over time, which is important for practically ensuring stability and convergence.

Weighing Q by $\dot{\text{œ}}_{\max}$ informs the application of **control effort** such that the "most difficult" orbital elements are addressed first, and ensures that no orbital element gets left behind.

$\dot{\text{œ}}_{\max}$ can be computed from the variational equations of motion, and results in an analytical expression for the derivatives of Q. Note that when formulated in modified equinoctial elements, analytical approximations are used for $\dot{\text{œ}}_{\max}$ [10, 11].

Petropoulos' original paper has been built upon numerous times for different applications, including rendezvous [11]. Varga and Pérez (2016) [10] give an implementation in modified equinoctial elements, along with a study on optimizing the values of $W_\sigma, \sigma \in \{P, a, e, i, \Omega, \omega\}$. Proceeding work on the Q-Law has adopted the modified equinoctial element formulation [11] for its better performance.

The Q-Law family has demonstrated remarkably good performance when tested in higher fidelity studies, incorporating eclipse effects (i.e. rendering electric propulsion inoperable when occluded from sunlight), and J2 perturbation [10]. Although solar sails are a relatively fresh application for this type of guidance law, the long history of good performance under challenging conditions makes it a good foundation to build upon for this project.

2.3 Considerations for Solar Sails

Solar sails are a propulsion method requiring no propellant expenditure to produce thrust. Their principle of operation is based on the conservation of momentum in the reflection of incident photons from the Sun. Challenges associated with performing controlled maneuvers using solar sails are described, with discussions of implications on spacecraft guidance. Fundamental principles are taken with reference to McInnes (1999) [7].

The most challenging aspects of bringing solar sails into reality are not actually related to trajectory planning; truthfully, the greatest issues lie in the manufacturing and production of solar sails; material science and mechanical design remain the greatest barriers to the widespread adoption of solar sails [7]. On top of that, attitude control is a fundamental precursor to thrust control, and is still in a highly developmental stage [23].

With that said, guidance is still an important and challenging problem for solar sailing. An important fact to consider is that real solar sails behave very differently from an ideal flat sail. As discussed by Polyakhova (2018) in a review of solar sailing missions, models describing the thrust produced by solar sails continue to change with every new spacecraft built and flown [24].

In a perfectly idealized model, thrust is produced exactly in the direction of the sail normal, and the cone angle can be as great as 90°. Real solar sails have limits on maximum allowable cone angle due to considerations for attitude control or because the reflective material of the sail behaves non-ideally at shallow incidence angles (e.g. absorption and re-radiation effects). Due to these same reflectivity effects, the resultant thrust vector is not always aligned perfectly with the sail normal. This is illustrated in Figure 2.2 below.

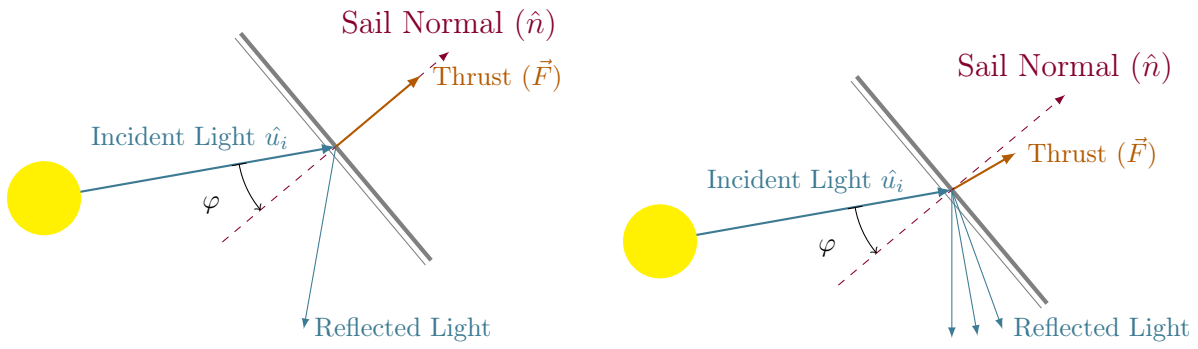

(a) Perfectly reflecting sail.

(b) Real sail.

Figure 2.2: Effects of non-ideal effects on solar sail thrust production.

2.3.1 Inherent Challenges of Thrust Production

Even in the case of a flat perfectly reflecting sail, there are two key obstacles complicating the application of low-thrust guidance theory to solar sail spacecraft.

1. **Direction-Dependent Availability of Thrust**: The thrust produced by a solar sail is related to the cone angle φ by a factor of roughly $\cos^2(\varphi)$ (see Equation 2.22 of Ref. [7]). Thrust falls off considerably as the sail becomes misaligned with the direction of incident light, and drops to zero for $|\varphi| > 90°$. This means that at any instant in time, only a single hemisphere of thrust directions can be realized, with the orientation of the hemisphere being dependent on the position of the Sun – a quantity that cannot be directly controlled. This is illustrated in Figure 2.3a.

2. **Time/Position-Dependent Availability of Thrust**: The availability of thrust depends on a clear line of sight to the Sun. In eclipse, no light hits the sail, and no thrust is produced. This is illustrated in Figure 2.3b. For spacecraft in low orbits above a planet, the time spent in eclipse represents a substantial fraction of the orbital period. More importantly, for a planetocentric orbit, the position of the parent planet around the Sun directly affects the direction of incident sunlight hitting the spacecraft and hence directional thrust availability. This is revisited in Section 2.4.

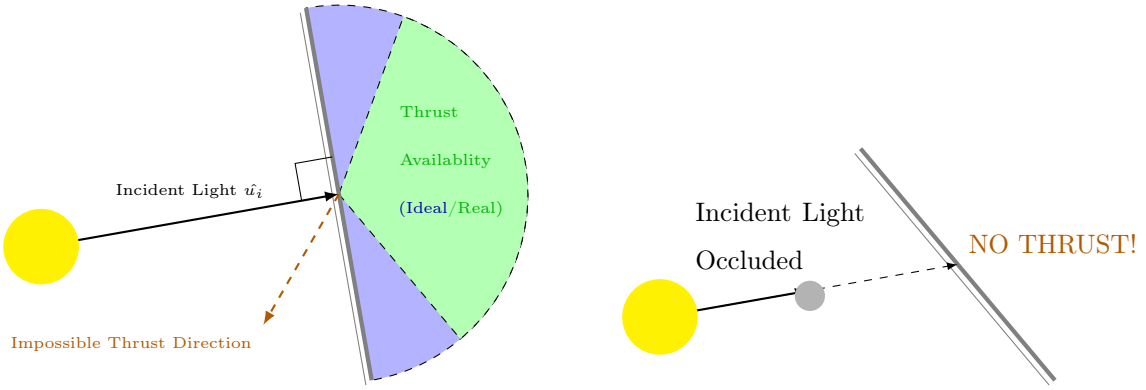

(a) The direction of produced thrust is limited for solar sails.

(b) Solar sails produce no thrust in eclipse.

Figure 2.3: Key challenges associated with solar sail thrust.

Both of these effects are present to a lesser degree in spacecraft using electric propulsion; solar arrays require Sun exposure but are typically made to rotate so that they can track the Sun independently of the direction of the engines. Solar sails pose a more extreme set of challenges for maneuvering, stemming from their principle of operation.

2.3.2 Diversity of Sail Geometries and Materials

McInnes (1999) [7] discusses several different solar sail geometries and reflectivity models with considerably different forms.

Real solar sails do not adhere to perfectly flat geometries due to deformation effects [25], and can even be designed intentionally with non-flat geometry for enhanced attitude control capabilities [26].

IKAROS (2010) featured variable-reflectivity materials on its surface for attitude control [27], and sail materials are an ongoing field of development, as discussed in a review of the state of the art by NASA (2011) [28].

The key point to be made is that fixating upon a certain dynamic model for solar sails is overly restrictive for adequate consideration of future solar sail designs.

Note that there is work done by Rios-Reyes et al. (2005) [29] and Tsunda et al. (2013) [30] on generalizing solar sail dynamics models. These models allow for arbitrary geometries and surface reflectivity properties but have a large number of parameters. For the sake of simplicity, integrating such a model into the guidance law for this project is not considered.

2.3.3 Attitude Dynamics

Solar sail spacecraft have limited attitude agility; as a first approximation, angular rates of about 15° per hour are achievable [23]. Even with this crude notion of maneuverability, maneuvers in orbits where the orbital period is shorter than a few hours (such as LEO) become difficult with solar sail spacecraft. Such considerations should be made when making a guidance law so that the time history of commanded thrust directions can be realized by the attitude controller.

Incorporating attitude constraints is complex; attitude control often depends on radiation pressure for maneuvering (e.g. tip vanes, LCD panels), and hence the maximum attainable attitude rates vary with the orientation of the spacecraft. Also, as previously mentioned, there are limits imposed on the angles of the sail relative to the Sun, which continuously vary in time as the Sun moves.

Considering attitude dynamics in a globally optimal method is challenging since the above constraints often cannot be expressed in a simple form. Even with feedback methods, directly incorporating such constraints into a guidance law dramatically increases its complexity.

Therefore, the majority of approaches to solar sail guidance make simplifications to ignore certain aspects of attitude dynamics.

2.4 Solar Sail Guidance

Traditional solar sail guidance has focused on heliocentric trajectories. Analytical analysis of inward and outward spiral trajectories around the Sun are discussed by McInnes (1999) [7]. However, the focus of this literature review is on planetocentric orbital maneuvering.

In planetocentric orbits, the issues of directional thrust availability and eclipse are more severe than when around the Sun. For instance, the "hemisphere" of allowable thrust directions (see Figure 2.3a) makes a full revolution during each orbit around the Sun, and therefore a solar sail in heliocentric orbit can apply thrust in nearly all directions over the course of a single orbit. On the other hand, the position of the Sun relative to a spacecraft barely changes throughout a single orbit around a planet, which greatly restricts the possible space of thrust directions. Consider Figure 2.4 for an illustration of this. Furthermore, as already mentioned, eclipse is a common occurrence in low orbit around a planet, while it is effectively nonexistent when orbiting the Sun.

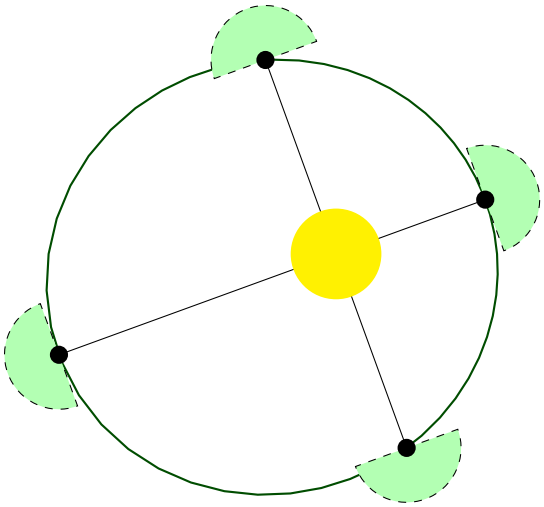

(a) Heliocentric trajectories: thrust availability depends only on the orientation of the spacecraft orbit relative to its parent body (the Sun).

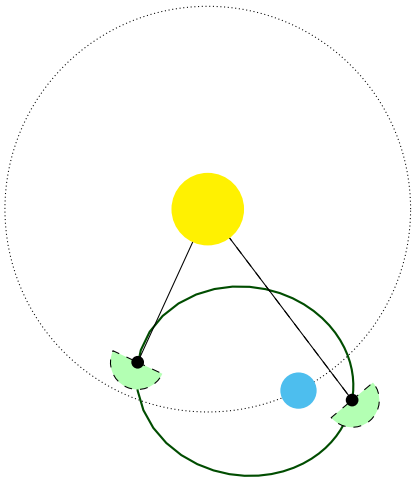

(b) Planetocentric trajectories: thrust availability also depends on the position of the parent planet around the Sun.

Figure 2.4: Differences between heliocentric and planetocentric solar sail flight.

2.4.1 Specialized Laws for Planetocentric Orbital Maneuvers

As discussed by Polyakhova (2018) [24], there are numerous applications of solar sails in Earth orbit, including orbit raising, de-orbiting, and sending spacecraft onto escape trajectories. For each of these applications, a specialized guidance law can be developed.

Coverstone and Prussing (2003) [5] present a feedback guidance law for escaping Earth from a geosynchronous transfer orbit. The technique employed is most similar to thrust-blending guidance laws, in which the rate of change of orbital energy is maximized. This guidance law performs to within the correct order of magnitude (in terms of time of flight) for a minimum-time escape, and demonstrates the utility of feedback guidance laws in planetocentric orbits. This guidance law performs a very specific task of sending a spacecraft onto an escape trajectory, solving the guidance problem for a special case of final orbit.

Fieseler (1998) [4] discusses a scheme for orbit raising which simply applies thrust along the velocity vector of the solar sail. This is taken as the core of a design featuring angled flaps to direct thrust in a prograde direction without incurring excessive atmospheric drag in low Earth orbit. This guidance scheme does not allow for targeting of a specific orbit, and a more sophisticated guidance law would need to be used once the orbit is raised to a point where drag is negligible.

2.4.2 Generalized Orbital Maneuvering

The overall field of planetocentric orbital maneuvering using solar sails is much less studied than the general low-thrust case. There are very few examples of guidance laws for maneuvering between arbitrary orbits around a planet.

One of the oldest approaches to this problem is presented by Sackett (1977) [31], using an indirect global optimization approach. This work produced examples of both orbit-to-orbit transfers, as well as escape trajectories. A key concern with the results of this work was the generation of unrealistic trajectories that flew very close to or into the Earth's surface.

MacDonald and McInnes (2005) [32] were among the first to formulate a contemporary feedback guidance law for orbital maneuvering. Their approach was to use a feedback guidance law using thrust-blending. This was the first use of a penalty function to prevent the spacecraft from plunging into the Earth.

The most recent development in the field is a paper from Oguri (2023) [12], which adapts the Q-Law for use with solar sails, by incorporating a popular sail reflectivity model into

the guidance law (done by incorporating sail thrust into the $\dot{oe}_{max}$ terms of Q). This work demonstrated that the remarkable performance of the Q-Law could be readily transferred to solar sails given adequate consideration for solar sail dynamics.

2.5 Research Gap and Approach

Given the robustness of the Q-Law to disturbances in environment and dynamics, it is interesting to consider an approach similar to that taken by Oguri (2023) [12], except without needing to incorporate solar sail dynamics directly into the derivatives of Q.

The ingredients for such an approach are already well-established, and the prospect of demonstrating good performance of a guidance law with a more general form appears feasible.

The choice of a Lyapunov-based feedback guidance law is supported by a healthy lineage of research in low-thrust spacecraft guidance, and the inclination to keep the guidance law as general as possible is motivated by the ongoing evolution of solar sail spacecraft designs and dynamics models.

Considering attitude dynamics for solar sails may be very complex, so it is favourable to ignore certain aspects such as rate limitations in developing the guidance law.

The direction is now well defined: create a solar sail guidance law for planetocentric maneuvering while keeping it very simple.

Chapter 3

Problem Formulation and Implementation

The formulation of the guidance law is presented in this chapter, including a full overview of the underlying Q-Law and the novel modifications made for solar sails. Before that, the problem is described in greater detail.

3.1 Problem Definition and Assumptions

The objective of this project is to develop a feedback guidance law for transferring between two orbits around a planet in orbit around the Sun using a solar sail spacecraft.

Stated more formally, the problem is given as:

Planetocentric Solar Sail Feedback Guidance Problem
Consider a spacecraft propelled by an ideal flat solar sail with sail loading σ and efficiency η in an ideal 2-body orbit around a planet with gravitational parameter μ (which itself orbits the Sun). Let be P the radiation pressure of incident sunlight, which comes from a known direction $\hat{u}_i$.
Given the instantaneous spacecraft state $\{p, f, g, h, k, L\}$ and target orbit described by the elements $\{\hat{p}, \hat{f}, \hat{g}, \hat{h}, \hat{k}\}$, determine an instantaneous spacecraft orientation in the LVLH frame (i.e. the sail normal $\hat{n}$, presented in the form of steering angles α and β) which ultimately brings the spacecraft to the target orbit.

The terms of this statement are elaborated in the proceeding subsections.

3.1.1 Orbit and Environment

The spacecraft is assumed to be orbiting a planet, possessing an instantaneous state expressed in modified equinoctial elements $\{p, f, g, h, k, L\}$ (i.e. an osculating orbit). The spacecraft is targeting an orbit described in modified equinoctial elements, as $\{\hat{p}, \hat{f}, \hat{g}, \hat{h}, \hat{k}\}$

The position of the spacecraft with respect to the planet is given by the vector $\vec{r}$, and the absolute velocity of the spacecraft is given by $\vec{v}$.

Remark on Notation: Mathematical notation for vectors follows the vectrix convention, as used in Ref. [14]. Abstract vectorial quantities are written with the arrow above (e,g $\vec{u}$), and vectors expressed in a reference frame $\vec{\mathcal{F}}$ are written in boldface (e.g. $\boldsymbol{u}$). Unit vectors are given a special notation, written using a hat (e.g. $\hat{u}$).

Reference Frames

Two reference frames are used in this problem, defined in Table 3.1, based on common convention. The frame $\vec{\mathcal{F}}_I$ has its origin at the center of the planet, and is taken to be inertial. The $\vec{\mathcal{F}}_{\text{LVLH}}$ is attached to the spacecraft, and its orientation is defined by the position vector of the spacecraft and the plane of the orbit.

Frame Name	Symbol	x-direction	y-direction	z-direction
Inertial	$\vec{\mathcal{F}}_I$	Points in direction of Υ	Perpendicular to $\hat{x}_I$ in equatorial plane	$\hat{z}_I = \hat{x}_I \times \hat{y}_I$
LVLH	$\vec{\mathcal{F}}_{\text{LVLH}}$	$\frac{\vec{r}}{\|\|\vec{r}\|\|}$	$\frac{\vec{r}\times\vec{v}\times\vec{r}}{\|\|\vec{r}\times\vec{v}\times\vec{r}\|\|}$	$\frac{\vec{r}\times\vec{v}}{\|\|\vec{r}\times\vec{v}\|\|}$

Table 3.1: The frames involved, and their definitions.

Quantities related to the guidance law are expressed in the LVLH frame, including steering command outputs. This choice of frame is motivated by past formulations of the Q-Law, which are based on variational equations in the LVLH frame.

Sun The Sun is located at a position $\vec{r}_\odot$ with respect to the planet, and hence the vector going from the Sun to the spacecraft is given by $\vec{r} - \vec{r}_\odot$. The direction of incident light is therefore given by $\hat{u} = -\frac{\vec{r}-\vec{r}_\odot}{\|\|\vec{r}-\vec{r}_\odot\|\|}$.

A diagram describing the elements of the problem discussed so far is shown in Figure 3.1.

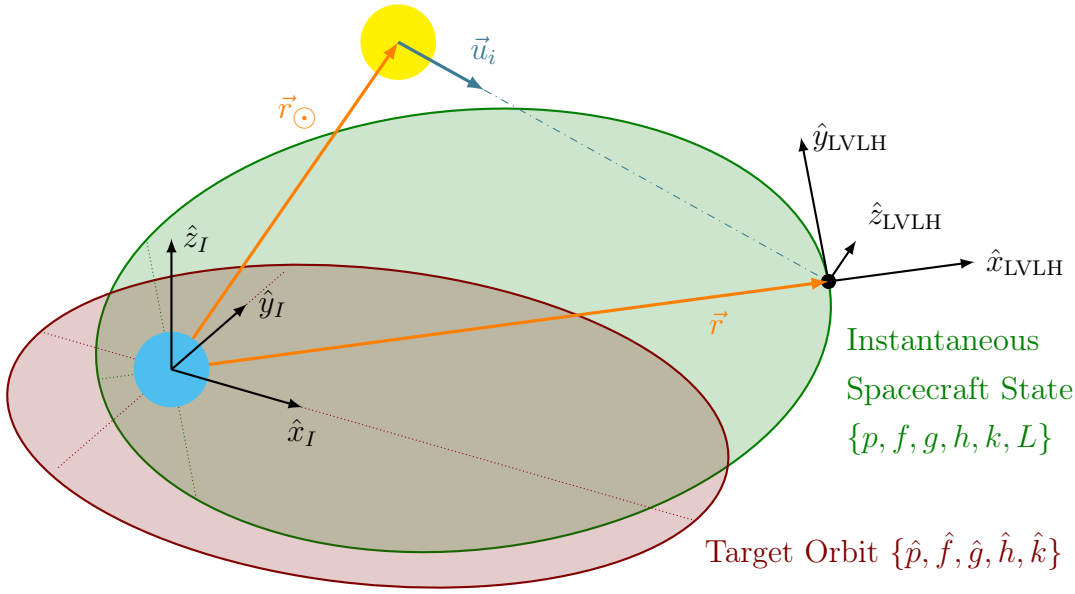

(a) Spatial setup of problem, primary view.

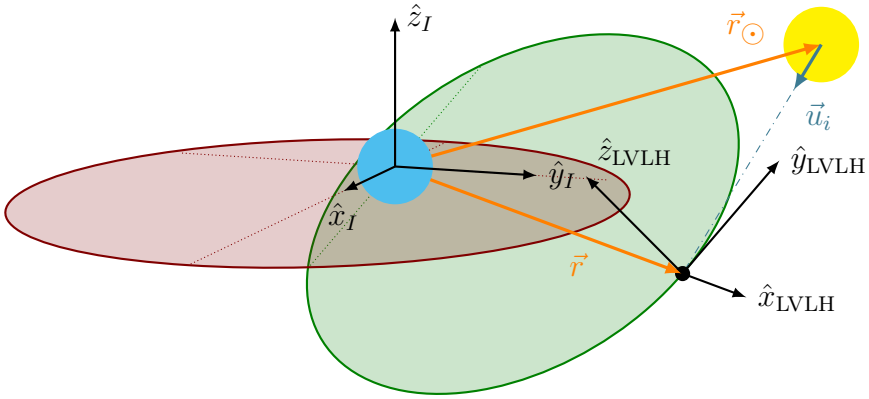

(b) Spatial setup of problem, alternate view.

Figure 3.1: Key elements of the problem (multiple views for clarity). The planet is represented by the blue circle, the Sun by the yellow circle, and the spacecraft by the black dot.

3.1.2 Spacecraft Orientation Convention

The output of the guidance law is a spacecraft orientation in the LVLH frame. That is, the guidance law expresses the unit vector $\hat{n}$ in terms of the output steering angles α and β.

The convention used in this project follows Refs. [9–11], and is depicted in Figure 3.2.

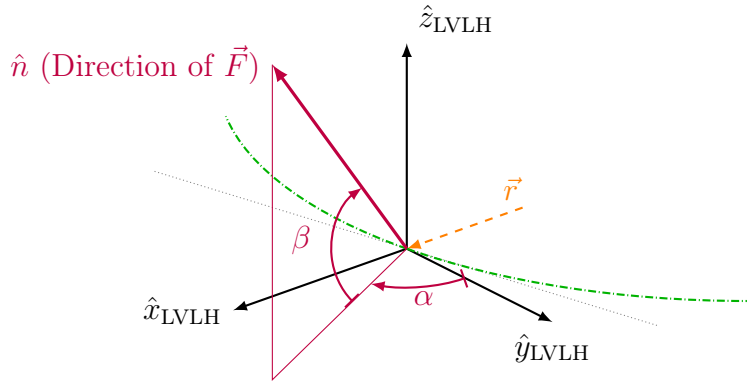

Figure 3.2: Thrust angle orientation convention. Note that generally, $\alpha = 0$ does NOT correspond to the direction of the velocity vector of the spacecraft, as $\vec{\mathcal{F}}_{\text{LVLH}}$ is aligned with $\vec{r}$ and $\vec{r} \times \vec{v}$. The dashed grey line represents the tangent line to the orbit, which is generally not aligned with $\hat{y}_{\text{LVLH}}$.

α is a clockwise steering angle from the y-axis in the xy LVLH plane, and β is a steering angle towards the $+z$ axis.

That is to say, the direction vector of the spacecraft is given by:

$$\hat{n}(\alpha, \beta) = \vec{\mathcal{F}}^{T}_{\text{LVLH}} \begin{bmatrix} \cos\beta \sin\alpha \\ \cos\beta \cos\alpha \\ \sin\beta \end{bmatrix} \tag{3.1}$$

3.1.3 Dynamics

Sail Thrust

Dynamics for an idealized flat solar sail are presented and used in the implementation of numerical simulations.

For a solar sail pointing in the direction $\hat{n}$ and for incident light in the direction $\hat{u}_i$, the acceleration imparted on the sail is given by:

$$\vec{F} = \frac{2P\eta}{\sigma}(\hat{u}_i \cdot \hat{n})^2 \ \text{sign}(\hat{u}_i \cdot \hat{n}) \ \hat{n} \ [\text{m s}^{-2}] \tag{3.2}$$

Where $P = 9.12 \times 10^{-6}\,\text{N m}^{-2}$ is the value of solar radiation pressure at a distance of 1 AU. The quantity $\sigma = \frac{m}{A}$ [kg m^{-2}] referred to as *sail loading* is the mass of the spacecraft divided by the sail area, and is conventionally used to parameterize sail performance. A dimensionless efficiency factor η represents "how reflective" the material of the sail is, relative

to a perfect reflector. The leading coefficient of 2 results from force imparted both by incident and reflected photons (see Figure 2.2a.)

Variational Equations of Motion

The equations of motion of the spacecraft in modified equinoctial orbital elements are given by (3.3) below.

$$\frac{\mathrm{d}}{\mathrm{d}t}\begin{bmatrix} p \\ f \\ g \\ h \\ k \\ L \end{bmatrix} = \frac{1}{q}\sqrt{\frac{p}{\mu}}\begin{bmatrix} 0 & 2p & 0 \\ q\sin L & (q+1)\cos L + f & -g(h\sin L - k\cos L) \\ -q\cos L & (q+1)\sin L + g & f(h\sin L - k\cos L) \\ 0 & 0 & \frac{\cos L}{2}(1+h^2+k^2) \\ 0 & 0 & \frac{\sin L}{2}(1+h^2+k^2) \\ 0 & 0 & h\sin L - k\cos L \end{bmatrix}\begin{bmatrix} F_r \\ F_\theta \\ F_n \end{bmatrix} + \begin{bmatrix} 0 \\ 0 \\ 0 \\ 0 \\ 0 \\ \frac{q^2\sqrt{\mu p}}{p^2} \end{bmatrix} \tag{3.3}$$

$$\text{with} \quad q \equiv 1 + f\cos L + g\sin L$$

F_r, F_θ, F_n correspond to perturbing accelerations on the spacecraft expressed in the LVLH frame corresponding to the radial, tangential, and normal directions respectively. That is:

$$\vec{F} = \vec{\mathcal{F}}^T_{\text{LVLH}}\begin{bmatrix} F_r \\ F_\theta \\ F_n \end{bmatrix}$$

3.1.4 Motion of the Sun

The sun is assumed to be 1.5×10^8 m from the center of the coordinate system, at an angle varying by 2π in 1 year ($\tau = 365.25\,\mathrm{d} = 31\,557\,600\,\mathrm{s}$).

That is,

$$\vec{r}_\odot(t) = 1.5 \times 10^8\ \vec{\mathcal{F}}^T_I\begin{bmatrix} \cos(\lambda_\odot) \\ \sin(\lambda_\odot)\cos(\varepsilon) \\ \sin(\lambda_\odot)\sin(\varepsilon) \end{bmatrix}\mathrm{m} \tag{3.4}$$

Where $\lambda_\odot = \frac{2\pi}{\tau}t$, with $t = 0$ corresponding to the vernal equinox, and $\varepsilon = 23.439°$ is the obliquity of the ecliptic.

This is obviously not reflective of Earth's elliptical orbit around the Sun, but it is assumed to be adequate as a starting point.

In this analysis, the position of the Sun is considered to be **quasi-static**, that is, $\dot{\lambda}_\odot = 0$, since the motion of the Sun occurs on a timescale much longer than the period of an orbit.

3.2 Methodology

The guidance law is implemented in a two-stage architecture, depicted in Figure 3.3 below. This choice is discussed more in the proceeding sections.

The guidance law occupies the left half of the diagram (blocks in blue and green), while the rest of the dynamics are shown in the purple blocks on the right.

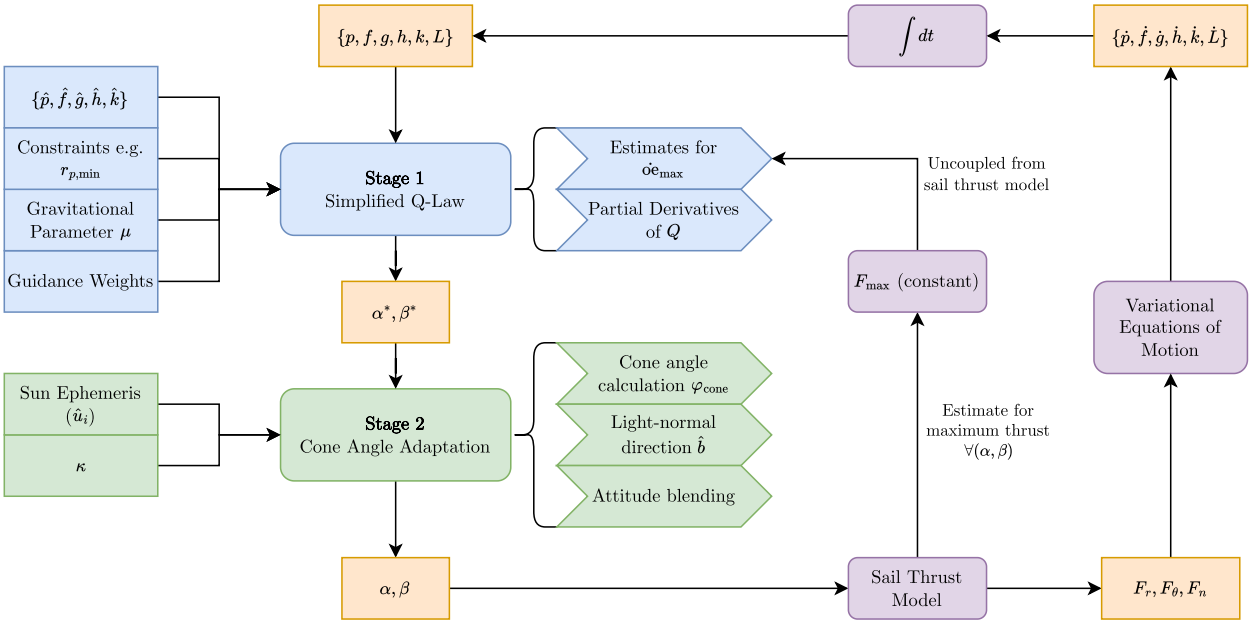

Figure 3.3: Architecture of the guidance law, along with the dynamics of the spacecraft.

The key idea of the overall approach taken in this project is to separate solar sail-related considerations (direction of incident light, restrictions on orientation) as much as possible from the Q-Law. The Q-Law stage of the guidance law **treats the solar sail as if it were a conventional low-thrust spacecraft** capable of producing an acceleration $F_{\max}$ in **all directions**. From this, it generates idealized angles α^*, β^*, which are then adapted by the second stage to make them feasible for a solar sail.

Rather than try to rework the Q-Law with solar sail dynamics like Ref. [12], this approach sticks with the conventional low-thrust guidance origins of the Q-Law; the cone angle adaptation block can be thought of as being **part of the dynamics**, with the Q-Law operating as if it were controlling a regular low-thrust spacecraft of acceleration $F_{\max}$.

3.3 Formulation of Simplified Q-Law

The simplified Q-Law is derived in this section, along with a computational procedure for assembling the steering angle outputs.

3.3.1 Control-Lyapunov Function

The simplified Q-Law is structured very similarly to previous works (Refs. [9–11]), following a control-Lyapunov function Q, which is then differentiated in terms of steering angles α, β to determine the thrust direction maximizing $-\dot{Q}$.

The control-Lyapunov function is given below in Equation 3.5.

$$Q = (1 + W_P P) \sum_{\text{œ}} W_{\text{œ}} S_{\text{œ}} \left(\frac{\text{œ} - \hat{\text{œ}}}{\dot{\text{œ}}_{\max[\alpha,\beta,L]}} \right)^2 \quad \text{œ} \in \{p, f, g, h, k\} \tag{3.5}$$

$$S_{\text{œ}} = \begin{cases} \frac{1}{R_e} & \text{œ} = p \\ 1 & \text{Otherwise} \end{cases}$$

$$P = \exp\left[\gamma \left(1 - \frac{r_p}{r_{p,\min}} \right) \right]$$

$$a = \frac{p}{1 - e^2}$$

$$r_p = a(1 - e) = p \frac{(1 - e)}{(1 + e)(1 - e)} = \frac{p}{1 + \sqrt{f^2 + g^2}}$$

with $\dot{\text{œ}}_{\max[\alpha,\beta,L]}$ being taken to mean the maximum achievable rate of change in that orbital element for any value of steering angles (α, β) and true longitude L.

The only variables in Q are $\text{œ} \in \{p, f, g, h, k\}$, and therefore Q can be written as a sum of derivatives using the chain rule:

$$\dot{Q} = \sum_{\text{œ}} \frac{\partial Q}{\partial \text{œ}} \dot{\text{œ}}$$

Note that Equation 3.3 in fact gives $\dot{\text{œ}}$ as a function of F_r, F_θ, F_n. The idea then is to link $\dot{Q}$ to the thrust model for the solar sail, without being overly specific. The key decision taken in deriving the Q-Law portion of the guidance law is to **assume that the solar sail always produces its maximum possible thrust in any direction** (i.e. Figure 3.4). Hence, Equation 3.6 is taken to be true (rather than Equation 3.2) for deriving ideal steering angles.

$$\begin{bmatrix} F_r \\ F_\theta \\ F_n \end{bmatrix} = \frac{2P\eta}{\sigma} \begin{bmatrix} \cos\beta \sin\alpha \\ \cos\beta \cos\alpha \\ \sin\beta \end{bmatrix} \equiv F_{\max} \begin{bmatrix} \cos\beta \sin\alpha \\ \cos\beta \cos\alpha \\ \sin\beta \end{bmatrix} \tag{3.6}$$

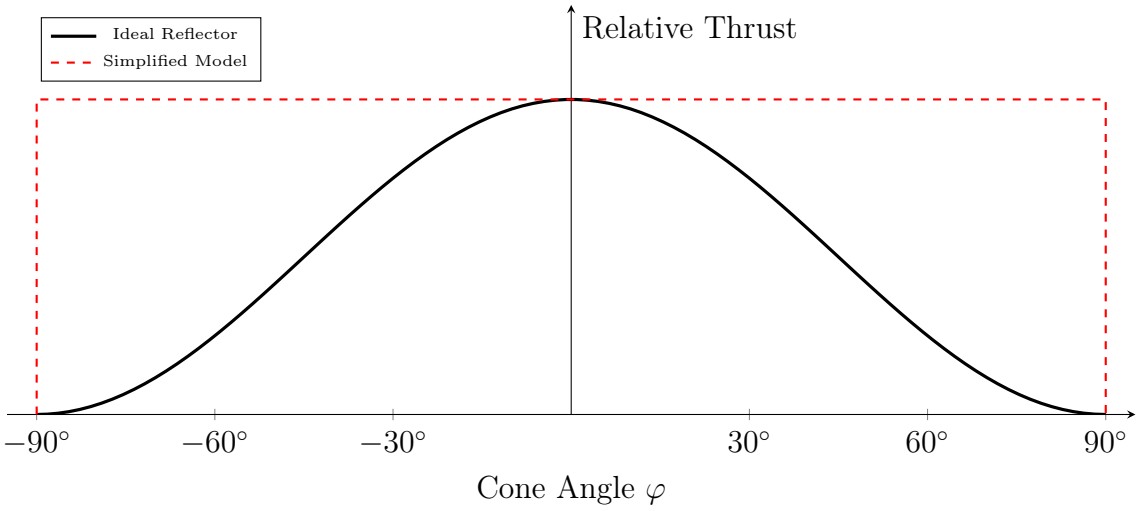

Figure 3.4: A significant assumption being made for the Q-Law portion of the guidance law is to remove the direction-dependence on produced thrust.

Keeping the relationship simple using only $F_{\max}$ allows for a very general application of the guidance law to a broad range of spacecraft configurations.

3.3.2 Ideal Steering Angles

By simultaneously considering Equations 3.3 and 3.6, $\dot{\text{oe}}$ becomes a function of α and β.

$\dot{Q}$ can therefore be expressed in a form based on steering angles, shown below:

$$\dot{Q} = D_1 \cos\beta \sin\alpha + D_2 \cos\beta \cos\alpha + D_3 \sin\beta \tag{3.7}$$

For some D_1, D_2, D_3 based on other variables/parameters. Finding the stationary point of $\dot{Q}$ with respect to (α, β) gives:

$$\alpha^* = \text{atan2}\left(-D_1, -D_2\right) \tag{3.8}$$

$$\beta^* = \text{atan2}\left(-D_3, \sqrt{D_1^2 + D_2^2}\right) \tag{3.9}$$

which maximizes $-\dot{Q}$. This form is obtained from Ref. [10], where the definitions of D_1 and D_2 are swapped compared to this project. The reasoning behind the ordering here is such that D_1, D_2, D_3 line up with F_r, F_θ, F_n.

3.3.3 Assembling the Guidance Output

The remaining piece consists of deriving expressions for all of the terms in Q and $\dot{Q}$ and assembling them to produce optimal steering angles.

Expressions for $\dot{\text{œ}}_{\max[\alpha,\beta,L]}$

$\dot{f}_{\max[\alpha,\beta,L]}$ and $\dot{g}_{\max[\alpha,\beta,L]}$ are taken as approximate analytical forms, first developed by Ref. [10]. The other 3 orbital elements have exact analytical expressions for maximum rate of change, obtained by manipulating Equation 3.3.

$$\dot{p}_{\max[\alpha,\beta,L]} = \frac{2p}{q}\sqrt{\frac{p}{\mu}}F_{\max}$$

$$\dot{f}_{\max[\alpha,\beta,L]} \approx 2F_{\max}\sqrt{\frac{p}{\mu}} \qquad \dot{g}_{\max[\alpha,\beta,L]} \approx 2F_{\max}\sqrt{\frac{p}{\mu}}$$

$$\dot{h}_{\max[\alpha,\beta,L]} = \tfrac{1}{2}F_{\max}\sqrt{\frac{p}{\mu}}\frac{1+h^2+k^2}{\sqrt{1-g^2+f}} \qquad \dot{k}_{\max[\alpha,\beta,L]} = \tfrac{1}{2}F_{\max}\sqrt{\frac{p}{\mu}}\frac{1+h^2+k^2}{\sqrt{1-f^2+g}}$$

Partials of Q

Each partial derivative of Q can be written as:

$$\frac{\partial Q}{\partial \text{œ}} = W_{\text{œ}}S_{\text{œ}}\left[W_P\frac{\partial P}{\partial \text{œ}}\left(\frac{\text{œ}-\hat{\text{œ}}}{\dot{\text{œ}}_{\max[\alpha,\beta,L]}}\right)^2 + 2(1+W_P P)\left(\frac{\text{œ}-\hat{\text{œ}}}{\dot{\text{œ}}_{\max[\alpha,\beta,L]}}\right)\right] \quad \text{œ} \in \{p,f,g,h,k\}$$

The final forms of D_1, D_2, D_3 can now be computed from this, with a few shorthands introduced for convenience:

$$\boldsymbol{\Xi}_E = \left[2\left(\frac{\text{œ}-\hat{\text{œ}}}{\dot{\text{œ}}_{\max[\alpha,\beta,L]}}\right)\right]_{\text{œ}\in\{p,f,g,h,k\}} \in \mathbb{R}^5$$

$$\boldsymbol{\Xi}_P = \left[\frac{\partial P}{\partial \text{œ}}\left(\frac{\text{œ}-\hat{\text{œ}}}{\dot{\text{œ}}_{\max[\alpha,\beta,L]}}\right)^2\right]_{\text{œ}\in\{p,f,g,h,k\}} \in \mathbb{R}^5$$

$$W = \text{diag}\left(\left[W_{\text{œ}}\right]_{\text{œ}\in\{p,f,g,h,k\}}\right) \in \mathbb{R}^{5\times 5}$$

$$S = \text{diag}\left(\left[S_{\text{œ}}\right]_{\text{œ}\in\{p,f,g,h,k\}}\right) \in \mathbb{R}^{5\times 5}$$

$$A = \begin{bmatrix} 0 & 2p & 0 \\ q\sin L & (q+1)\cos L + f & -g(h\sin L - k\cos L) \\ -q\cos L & (q+1)\sin L + g & f(h\sin L - k\cos L) \\ 0 & 0 & \frac{\cos L}{2}(1+h^2+k^2) \\ 0 & 0 & \frac{\sin L}{2}(1+h^2+k^2) \end{bmatrix} \in \mathbb{R}^{5\times 3}$$

(q is defined in Equation 3.3).

$$\boldsymbol{D} = \begin{bmatrix} D_1 \\ D_2 \\ D_3 \end{bmatrix} \in \mathbb{R}^3$$

Combining everything together gives:

$$\boldsymbol{D} = \begin{bmatrix} D_1 \\ D_2 \\ D_3 \end{bmatrix} = A^T W S \left(W_P \boldsymbol{\Xi}_P + (1 + W_P P) \boldsymbol{\Xi}_E \right) \tag{3.10}$$

Combined with Equations 3.8 and 3.9, this gives a computational procedure for the ideal steering angles.

Additionally, $\dfrac{\partial P}{\partial \text{œ}}$ is calculated using symbolic algebra, with expressions shown below. They are rather ugly, but presented for completeness.

$$\frac{\partial P}{\partial p} = -\frac{k}{r_{p,\min}\left(\sqrt{f^2+g^2}+1\right)} \exp\left[-k\left(\frac{p}{r_{p,\min}\left(\sqrt{f^2+g^2}+1\right)} - 1\right)\right]$$

$$\frac{\partial P}{\partial f} = f\frac{pk}{r_{p,\min}\left(\sqrt{f^2+g^2}+1\right)^2\sqrt{f^2+g^2}} \exp\left[-k\left(\frac{p}{r_{p,\min}\left(\sqrt{f^2+g^2}+1\right)} - 1\right)\right]$$

$$\frac{\partial P}{\partial g} = g\frac{pk}{r_{p,\min}\left(\sqrt{f^2+g^2}+1\right)^2\sqrt{f^2+g^2}} \exp\left[-k\left(\frac{p}{r_{p,\min}\left(\sqrt{f^2+g^2}+1\right)} - 1\right)\right]$$

$$\frac{\partial P}{\partial h} = 0$$

$$\frac{\partial P}{\partial k} = 0$$

3.4 The Simplified Q-Law Alone is Insufficient

A solar-sail-agnostic formulation of the Q-Law is insufficient as a solar sail guidance law on its own. Two notable problem cases arise from ignoring solar sail attitude constraints:

(a) The Q-Law can request a thrust direction which points *towards* the Sun, resulting in reverse thrust. This causes the guidance solution to become unstable.

(b) The Q-Law can request a thrust direction pointing almost perpendicular to the direction of incident light, which, following Equation 3.2 produces nearly no thrust and stalls the progress of the solar sail.

These are illustrated in Figure 3.5.

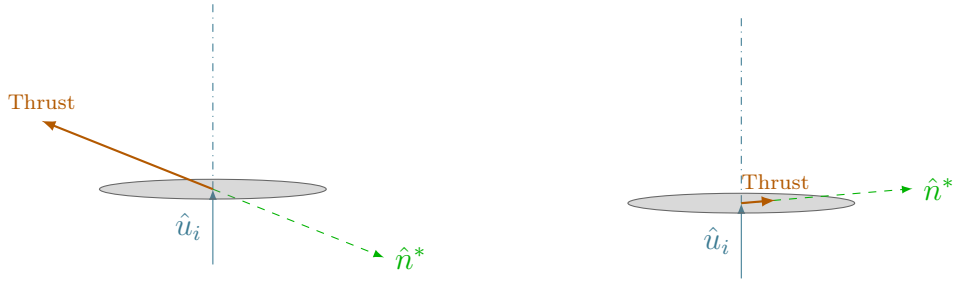

(a) $\varphi > 90°$ - Unstable. (b) $\varphi \approx 90°$ - No Progress.

Figure 3.5: Problematic cases associated with a solar-sail-agnostic guidance law.

Ignoring solar sail dynamics in the Q-Law portion of the guidance law simplifies the formulation, but comes at the cost of requiring an additional mechanism to overcome the above issues. The solution used in this project is to transform the desired thrust direction $\hat{n}^*$ into an "actual" thrust direction $\hat{n}$ by examining the cone angle associated with $\hat{n}^*$, and comparing it with what is achievable by the solar sail.

3.5 Cone Angle Adaptation Heuristic

The heuristic used to adapt the ideal steering angles from the simplified Q-Law stage is formulated in this section, beginning from the conceptual motivation of the idea.

3.5.1 Concept

If the cone angle produced by the ideal steering angles from the first stage is outside the achievable range of the solar sail, there are two options:

1. **Feather the sail**: Orient the solar sail (normal) at exactly 90° relative to the incident sunlight to produce zero thrust.
2. **Make a compromise**: Find the "closest" valid sail orientation, subject to the cone angle restriction. (This notion of "closeness" is elaborated upon in the formulation).

Feathering the sail is useful for situations where the cone angle suggested by the first stage exceeds 90° (i.e. the sail cannot produce thrust in that direction). This prevents the spacecraft from regressing **away** from its target orbit.

The latter option is particularly helpful even in the case of an ideal flat solar sail, where the first stage of the guidance law could produce a set of steering angles resulting in a cone

angle very close to 90°. The thrust produced in such a situation would be extremely small and result in less progress being made compared to if the guidance law accepted a thrust direction that does not point exactly towards the local optimum. By accepting a non-ideal direction, the spacecraft can still make progress toward its goal.

This highlights a counter-intuitive aspect of solar sail dynamics; it is sometimes favourable to point somewhere other than the desired direction of thrust so that a greater amount of total thrust (not necessarily in the desired direction) is produced. **Decreasing the cone angle of the sail can dramatically increase its thrust**, and this is the core idea of the cone angle adaptation heuristic.

3.5.2 Formulation

The ideal steering angles α^*, β^* are used to compute an idealized cone angle.

$$\varphi^* = \arccos(\hat{u}_i \cdot \hat{n}^*) \tag{3.11}$$

where $\hat{n}^* = \hat{n}(\alpha^*, \beta^*)$ can be computed using (3.1) and $\hat{u} = -\frac{\vec{r}-\vec{r}_\odot}{||\vec{r}-\vec{r}_\odot||}$. Both vectors are expressed in the same frame for computational procedures (e.g. the LVLH frame).

Consider an angle $\kappa \in [0° \, 90°]$ which is a guidance law parameter defining a cone in space called the *thrust cone*. The thrust cone has its axis coincident with $\hat{u}_i$, and is set such that any thrust direction laying within the cone produces a "large" amount of thrust.

Let the *limit plane* be the plane normal to $\hat{u}^i$. Consider a vector $\hat{b}$ which lies in the limit plane, e.g. $\hat{b} = \hat{u}_i \times (\hat{n}^* \times \hat{u}_i)$.

The resulting sail normal $\hat{n}$ is then calculated as:

$$\hat{n} = \begin{cases} \hat{n}^* & \cos\varphi^* > \cos\kappa \\ \cos\kappa \; \hat{u}_i + \sin\kappa \; \hat{b} & \cos\varphi^* \in [0, \cos\kappa] \\ \hat{b} & \cos\varphi^* < 0 \end{cases} \tag{3.12}$$

Or, in words:

- If the desired thrust direction lies within the thrust cone, use it as-is.
- If the desired thrust direction points away from the Sun but lies outside the thrust cone, project it upon the thrust cone, and use the resultant direction.
- If the desired thrust direction points towards the Sun, feather the sail.

This is illustrated more clearly in Figure 3.6.

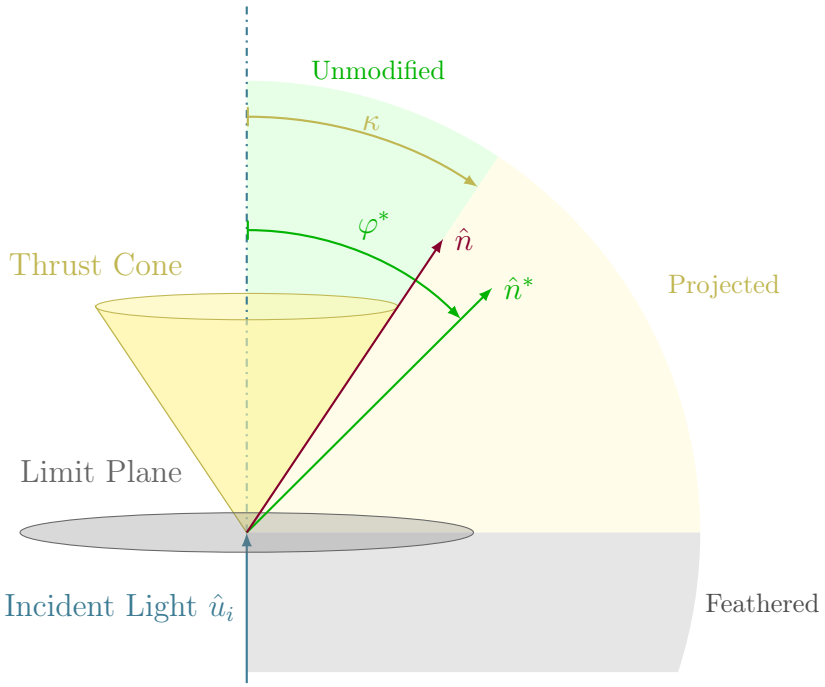

Figure 3.6: Overview of cone angle adaptation heuristic. The vertical is aligned with the direction of incident sunlight.

Figure 3.7 provides a visual depiction of all 3 cases.

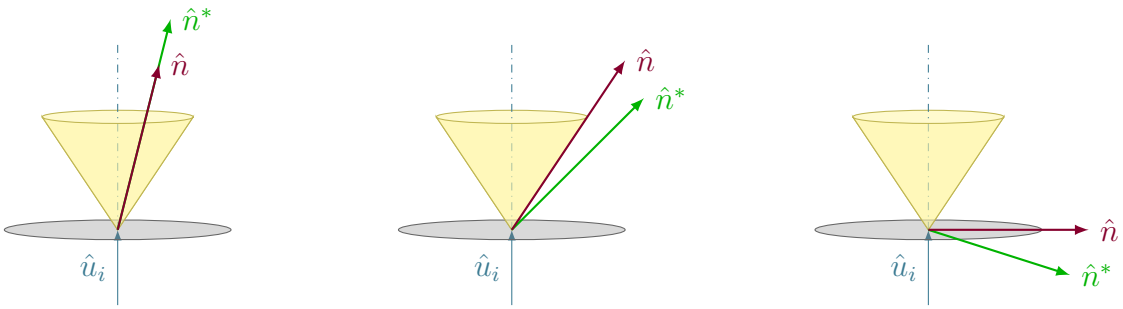

(a) Inside thrust cone; use Q-Law solution as-is.

(b) Outside of thrust cone; project $\hat{n}^*$ onto cone.

(c) Outside of limit plane; feather sail (no thrust).

Figure 3.7: The 3 different cases of the cone angle adaptation heuristic illustrated.

Both of the problematic cases from Section 3.4 are addressed with this adaptation heuristic. **This approach takes care of two birds with one cone.**

Setting the thrust cone angle κ is a matter of guidance strategy; as a starting point, it could be set to be equal to the absolute maximum allowable cone angle for a solar sail (e.g. 60° for a realistic solar sail), but it can also be set to an even lower angle to enforce greater production of thrust. This parameter is therefore decoupled from the solar sail thrust model used, and could readily be extended to a variety of spacecraft configurations.

Note that real solar sails which rely on solar radiation pressure for attitude control cannot feather themselves, but this formulation provides the basis for an approach wherein $\varphi^* > 90°$ could be taken to mean "reconfigure the spacecraft to produce zero (or almost zero) thrust".

3.6 Combined Guidance Law

The Q-Law and the cone angle adaptation heuristic form a combined guidance law. This guidance law is called QUAIL: Q-Law Using Angle of Incidence Limits.

Figure 3.8: QUAIL logo.

3.6.1 Properties of the Combined Guidance Law

One important formulation-level consequence of the approach taken by QUAIL is that the Lyapunov stability of the baseline Q-Law is **not** preserved.

1. The initial simplification made in the first stage of ignoring the direction-dependence of thrust production means that $\dot{\alpha}_{\max}$ is itself not calculated for a proper solar sail spacecraft, and so the formulation of $\dot{Q}$ does not correspond to the actual dynamics.

2. A stabilizing input may not always be provided since the thrust direction requested by the first stage can be altered by the second stage.

These two additions destroy the theoretical convergence guarantee of a control-Lyapunov function, meaning that Q may sometimes increase before it can decrease.

By relaxing the requirement that the spacecraft must always "improve" its trajectory, it can reposition itself into a state where more thrust is available in a certain direction, affording it greater "leverage". Consider Figure 2.4b, where it could be advantageous to wait until Earth has travelled to the opposite of the Sun from its current position to produce thrust in a direction that is currently inaccessible. By combining the Q-Law with the second stage cone angle adaptation heuristic, two very desirable properties are achieved:

1. The baseline Q-Law prioritizes correcting orbital elements with the largest error and/or smallest accessible rate of change.

2. The cone angle adaptation heuristic prioritizes directions in which the solar sail can produce thrust.

In combination, QUAIL attempts to first correct orbital elements which 1) require large corrections and 2) are accessible by the solar sail. This is a natural extension of the behaviour of the baseline Q-Law. Just like the Q-Law, any errors which are not immediately corrected are taken care of later, due to the feedback nature of the guidance law.

By removing the need for Q to be a true control-Lyapunov function, an extremely convenient method for producing an ideal thrust direction is obtained, and a very simple computational procedure is available for adapting this thrust direction into one usable by a solar sail. At the same time, a conceptually well-behaved guidance law is obtained.

3.6.2 Computational Procedure

Following the computation of (α^*, β^*) by the first stage, φ^* is computed using Equation 3.11. $\hat{n}^*$ is computed in referential form (i.e. its components are calculated relative to some reference frame), and the vector $\hat{b}$ is formed. Then, Equation 3.12 is used to calculate $\hat{n}$, using conditional expressions.

Expressing $\hat{n}$ in $\vec{\mathcal{F}}_{\text{LVLH}}$, the steering angles α and β can be found by working backwards from Equation 3.1. A reference formulation is given below:

$$\alpha = \text{atan2}\left(\hat{n} \cdot \hat{x}_{\text{LVLH}},\ \hat{n} \cdot \hat{y}_{\text{LVLH}}\right)$$
$$\beta = \text{atan2}\left(\hat{n} \cdot \hat{z}_{\text{LVLH}},\ \sqrt{(\hat{n} \cdot \hat{x}_{\text{LVLH}})^2 + (\hat{n} \cdot \hat{y}_{\text{LVLH}})^2}\right)$$

The problem statement at the beginning of this chapter is therefore solved by QUAIL.

Chapter 4

Implementation and Testing

Details about the implementation of QUAIL in simulation are presented in this chapter, including the test cases used to assess the performance of the guidance law.

4.1 Convergence Criterion

The previous chapter formulates the guidance law as a single-timestep operation, but in a simulator the guidance law is run many times to eventually reach some convergence threshold. The guidance law does not come "bundled with" an obvious convergence criterion; Q has units of time squared, but it would be preferable to have a dimensionless value for determining convergence. The criterion chosen was the following:

$$\delta = \sum_{\text{œ}} (\text{œ} - \hat{\text{œ}})^2 \quad \text{œ} \in \{\tilde{p}, f, g, h, k\}$$

where $\tilde{p} \equiv \frac{p}{R_e}$ (normalized by the radius of Earth) to render everything dimensionless. δ is compared to a preset tolerance to determine when to stop integration.

4.2 Implementation in Simulation

With reference to the architecture in Figure 3.3 and the procedures shown above, the complete guidance law and dynamics are implemented in two separate simulators.

Both simulators use very standard implementations of dynamics, and there is nothing particularly special about their inner workings. Brief descriptions are provided in this report, and the full source code is available for viewing.

4.2.1 MATLAB Implementation

Link to GitHub Repository

The MATLAB implementation, named "SLyGA" (Solar Lyapunov Guidance Algorithm) is the primary simulator used for analysis. The 3 most important parts of it are listed below:

1. **Simulator**: models the motion of a solar sail spacecraft.
   (a) **Dynamics**: Translational equations of motion in either Cartesian coordinate or modified equinoctial orbital elements. **Attitude dynamics are not considered.**
   (b) **Ephemerides**: Models the motion of the Sun around the Earth, using the simplified motion presented in (3.4). **In this study, all simulations have $t = 0$ corresponding to the vernal equinox**.
   (c) **Eclipse Model**: Detects when the Earth occludes the Sun and halts solar sail thrust production. Formulation based on [33], no penumbra included.
   (d) **Perturbation Model**: Adds J2 perturbations (can be toggled on and off).
   (e) **Propulsion Model**: Models ideal solar sail thrust and thrust from a conventional spacecraft. More detailed thrust models could be added similarly to the ones already implemented.
2. **Guidance**: Steering laws, notably QUAIL.
   (a) **Q-Law**: Implementation of the formulation given in the previous chapter.
   (b) **Cone Angle Adaptation**: Using the solar ephemeris, implements the formulation from the previous chapter.
3. **Case Files**: Provide initial conditions and parameters for test cases. The case files generate `struct` types containing the problem data, with fields presented in Table 4.1.

A post-processing suite built into SLyGA is used to generate plots and animations of the trajectories, shown in the next chapter.

MATLAB's built-in ODE integrators are mature and include a streamlined system for including events (used for terminating integration when converged). SLyGA is hence used for high-fidelity simulation cases. A key drawback of this implementation is its speed – simulation runs take around 10-60 seconds to complete. While it is fine for single runs, parametric sweeps require a faster solution.

Field Name	Description	Example Values
`y0`	Initial Orbital Elements (modified equinoctial elements $\{p, f, g, h, k, L\}$, p given in m)	`[20e6; 0.5; -0.2; 0.5; 0; 0]`
`y_target`	Target Orbital Elements $\{\hat{p}, \hat{f}, \hat{g}, \hat{h}, \hat{k}\}$	`[25e6; 0.2; 0.5; 0; 0.3]`
`propulsion_model`	Propulsion model function handle; thrust as a function of commanded thrust direction	`@sail_thrust`
`steering_law`	Guidance law function handle; steering angles as a function of current and target states	`@quail`
`guidance_weights`	W_{oe} in the Q-Law	`[1; 1; 1; 1; 1]`
`penalty_param`	γ in the Q-Law	`1`
`min_pe`	$r_{p,\text{min}}$ in the Q-Law (m)	`10000e3`
`penalty_weight`	W_p in the Q-Law	`0`
`kappa`	κ in cone angle adaptation	`deg2rad(60)`
`solver`	ODE solver for integration	`@ode89`
`t_span`	Integration timespan (s) – end time represents the maximum time allotted before a run is considered to not be converged	`[0, 1e8]`
`tol`	Termination tolerance, in terms of the sum of squares of errors between each orbital element	`1e-3`
`dynamics`	Switches between equations of motion in Cartesian coordinates and modified orbital elements	`"cartesian"`
`j2`	Switches $J2$ perturbation on and off	`true`

Table 4.1: Mission configuration structure for simulations.

4.2.2 C/Python Implementation

Link to GitHub Repository

The C/Python implementation, named "cshanty" (i.e. Sea Shanty) is built for tuning the weights of the guidance law. The C portion of the codebase contains all of the guidance law and dynamics, as well as a custom ODE integrator based on weights found by Verner [34]. The Python portion of the code wraps the C simulator into an interface for optimization using SciPy [35].

Dynamics are copied over from SLyGA in a 1:1 manner where possible, but certain more complex features are excluded. Notably, perturbations and eclipse modelling are absent. The implementation of guidance-related components is essentially the same as in MATLAB. Given that this implementation loses some fidelity, the primary use case for cshanty is to optimize cases developed for SLyGA. As such, cshanty is designed to accept case files in the same format as that depicted in Table 4.1.

The key benefit of a compiled implementation is speed; cshanty runs somewhere between 100 to 1000 times faster than SLyGA (about a few hundred milliseconds per run), meaning that parameter optimization runs can be performed in the span of a few hours.

4.3 Testing Methodology

The following list presents the testing repertoire used to assess the performance of QUAIL.

- **Baseline Cases**: Used to demonstrate that the guidance law works (is convergent) under a variety of challenging orbit-to-orbit transfer cases.
- **Extended Studies**: Used to probe the capabilities of QUAIL beyond the idealized baseline formulation.
  (a) **Time of Flight Optimization**: Attempting to recover global time optimality by tuning W_{oe}.
  (b) **Disturbance Rejection**: Seeing if QUAIL can still converge in the presence of orbital perturbations.
  (c) **Realistic Solar Sail Modelling**: Applying QUAIL to a crude model of a cone-angle-limited solar sail to see if it can work for realistic spacecraft.

4.4 Baseline Trajectory Cases

Four trajectory cases are developed to test the ability of QUAIL to perform planetocentric orbital transfers. These are presented in terms of an initial orbit and a target set of orbital elements. The initial and target orbital elements are given in Table 4.2.

Case ID		p $[1 \times 10^3\,\mathrm{m}]$	f	g	h	k	L [rad]
A	Initial	20 000	0.5	−0.2	0.5	0	0
	Final	25 000	0.2	0.5	0	0.3	N/A
B	Initial	11 625	0.725	0	0	0	0
	Final	42 165	0	0	0	−1	N/A
C	Initial	20 000	0.5	0	1	0	0
	Final	20 000	0.5	0	−1	0	N/A
D	Initial	42 164	0	0	0	0	0
	Final	42 464	0	0	Free	Free	N/A

Table 4.2: Baseline trajectory cases.

Free orbital elements are implemented by assigning a value of zero to the corresponding weight (i.e. $W_{\text{œ}} = 0$).

For each trajectory case, values of the guidance parameters used are presented in Table 4.3.

Case ID	W_P	γ	$r_{p,\min}[1 \times 10^3\,\mathrm{m}]$	W_p	W_f	W_g	W_h	W_k	κ
A	0	N/A	N/A	1	1	1	1	1	64°
B	1	5	6878	1	1	1	1	1	64°
C	1	1	10000	1	1	1	1	1	64°
D	0	N/A	N/A	5	0.5	1	0	0	64°

Table 4.3: Guidance parameters for each baseline trajectory case.

The details of each case are discussed briefly.

Case A: The "Everything Changing" Transfer

This case has no practical applicability, but tests QUAIL under a combined plane change, nodal rotation, and orbit raising. Executing this maneuver requires thrust in essentially all

directions, so it is a good test of the cone angle adaptation heuristic and its ability to provide thrust in all of the required directions.

Case B: Polar GSO Transfer

This case is based on "Case G" from [12], and is included as a test to see if QUAIL can perform the same types of transfers accomplished using other solar sail planetocentric guidance laws.

Case C: Plane Change

A 180° plane change maneuver is included to test the periapsis radius constraint of the guidance law, i.e. to see if the spacecraft crashes into the Earth or not. Another interesting point to probe is to see how "smoothly" the plane change is executed; conventional spacecraft perform the plane change roughly at a constant rate, but a solar sail may do so in spurts, owing to the direction-dependent availability of thrust.

Case D: GEO Disposal

Inspired by Hao Mei's research [36], a case is added to see if QUAIL can plan out trajectories for transferring from geostationary orbit to a GEO + 300 km graveyard orbit.

4.5 Extended Study: Time of Flight Optimization

The guidance parameters in Table 4.3 are a baseline. An important question that follows is whether a more time-optimal trajectory can be obtained through careful tuning of the guidance parameters.

A set of global optimization runs is performed to find the parameters yielding minimum time-of-flight.

4.5.1 Cone Angle Adaptation Heuristic Tuning

The value of κ is optimized using bounded univariate optimization through measured time-of-flight in case A. The value of κ in the interval $[30°, 85°]$ is determined using Brent's method [37].

The resultant optimum of $\kappa \approx 64°$ is used for proceeding analysis of all the other cases. Note that this is not an exact optimum for all of the other cases, but it provides a sufficiently good tradeoff between achieving high thrust and achieving thrust in the desired direction that it should be universally applicable.

4.5.2 Q-Law Parameter Tuning

All five weights $W_{œ}$, œ $\in \{p, f, g, h, k\}$ are optimized using a dual-annealing global optimization algorithm provided by SciPy [35]. Using $W_{œ}$ as the set of design variables, the time of flight resulting from simulation runs in the C simulator is used as the objective function to minimize.

A **stochastic optimization** scheme is chosen over a traditional gradient-based method because of the poor conditioning of the problem; for certain combinations of $W_{œ}$, the simulations do not converge, and in other cases, small variations in $W_{œ}$ cause sharp and extreme changes in time of flight. An annealing-based stochastic approach can work around these issues and return a globally optimal solution at the cost of extra runtime. Since the optimization runs only need to be performed once per case, the computational cost is considered tractable.

Only cases A and B are optimized for time of flight, as they are the more complex cases out of the four, and have the greatest potential for improvements.

4.6 Extended Study: Disturbance Rejection

The baseline dynamics model in SLyGA uses spherically symmetric gravity (i.e. $\vec{F} = -\frac{GMm}{||\vec{r}||^3}\vec{r}$), but oblateness effects are quite important for solar sail spacecraft, as acceleration from these perturbations represent a non-trivial fraction of the acceleration produced by thrust.

Using a standard formulation for $J2$ perturbation in modified equinoctial elements from [38], the second zonal harmonic effect is incorporated into the dynamics. A special test case is made using a LEO spacecraft (to increase the strength of perturbing accelerations), transferring from orbital elements shown in Table 4.4.

Case ID		p [1×10^3 m]	f	g	h	k	L [rad]
J	Initial	6878	0.1	−0.1	0	0	0
	Final	7500	0	0	0	0.2	N/A

Table 4.4: Special trajectory case for $J2$ perturbation.

Case ID	W_P	γ	$r_{p,\min}[1 \times 10^3\,\mathrm{m}]$	W_p	W_f	W_g	W_h	W_k	κ
J	2	1	6878	1	1	1	1	1	64°

Table 4.5: Guidance parameters for special case.

This special case represents a combined orbit raising and plane change maneuver, executed at an altitude of only 500 km above the surface. The periapsis penalty is hence also active.

4.7 Extended Study: Realistic Solar Sail Modelling

As a crude approximation to incorporating a realistic solar sail thrust model, a study is conducted on restricting κ, and seeing how restricting the maximum cone angle affects performance. Sweeping κ from 90° down to 10°, the impact on the time of flight for cases A and B is studied.

4.8 Computer and Software Environment

All simulation work is run on a Intel i7-7700HQ (2.80 GHz quad core) CPU with 16 GB of RAM on Windows 10, using MATLAB R2023a, Python 3.11, and GCC v8.1.0 (MinGW-W64).

Chapter 5

Results and Discussion

OUTCOMES of the simulation cases are presented. The performance of the guidance law is assessed based on performance in the numerical experiments. Consideration of the methodology is used to explain some of the observed behaviours, and deficiencies are noted for improvement.

5.1 Baseline Case Runs

The baseline trajectory cases outlined in Tables 4.2 and 4.3 were simulated, and the main results are shown in Table 5.1.

Case ID	Convergence Tolerance	Time of Flight (d)	# Revolutions	CPU Time (s)
A	0.001	621	862	17.6
B	0.03	498	501	16.9
C	0.005	802	1560	38.3
D	0.005	63	62	10.1

Table 5.1: Summary of outcomes for each case.

Case-by-case plots of the time history of the orbital elements and trajectories are shown in the proceeding sections.

5.1.1 Plots: Cases A-D

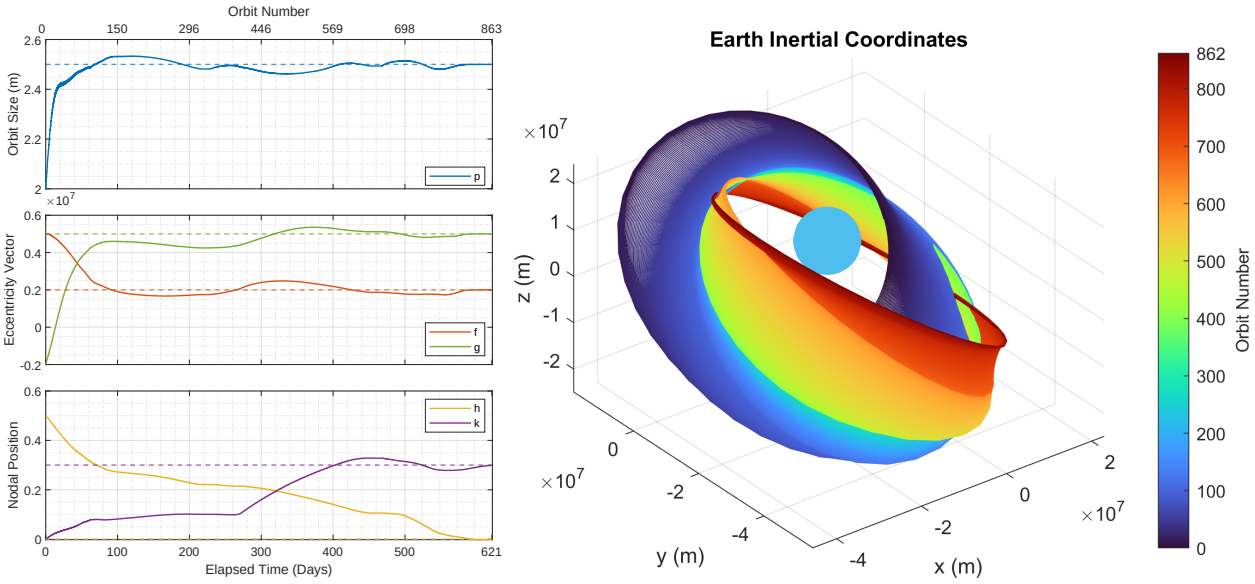

(a) Evolution of orbit elements in time. (b) Trajectory plot.

Figure 5.1: Orbital elements and trajectory for case A.

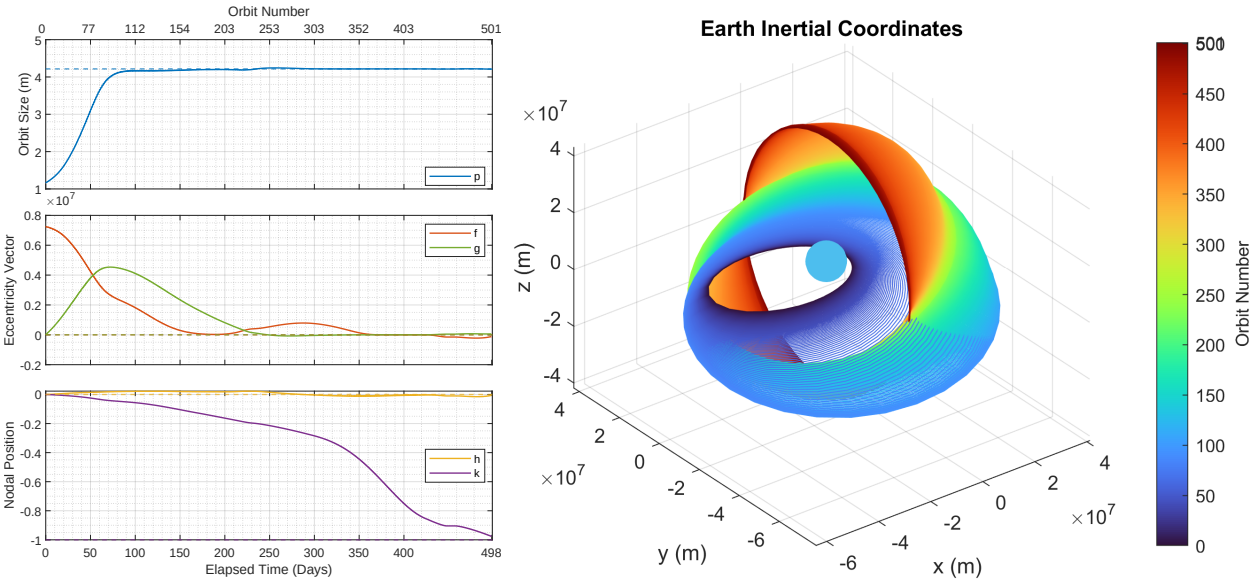

(a) Evolution of orbit elements in time. (b) Trajectory plot.

Figure 5.2: Orbital elements and trajectory for case B.

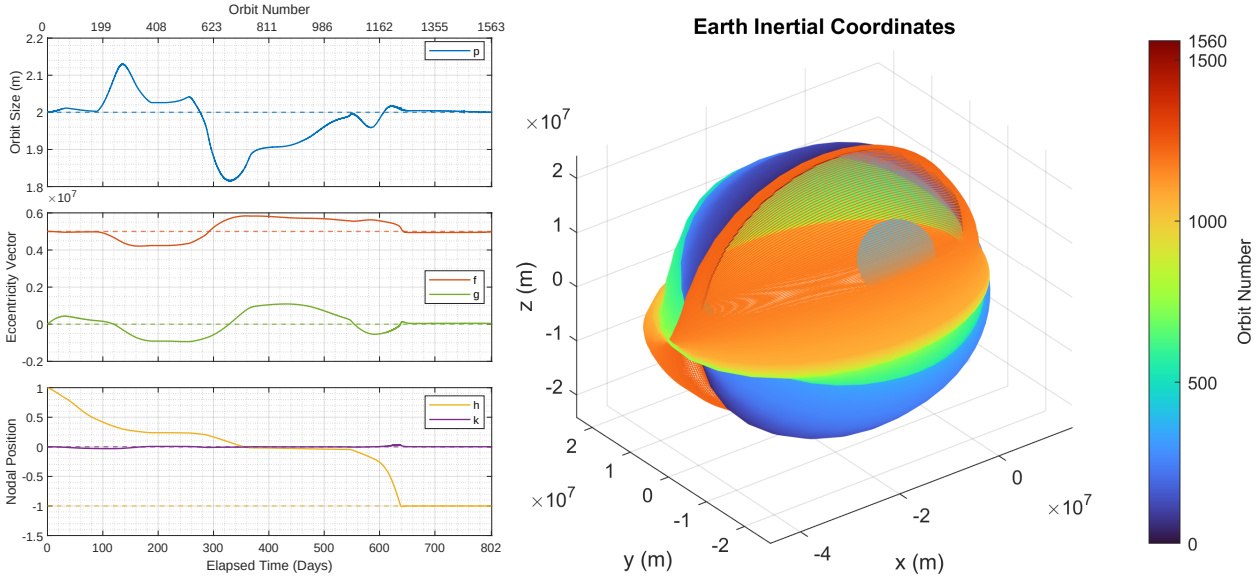

(a) Evolution of orbit elements in time. (b) Trajectory plot.

Figure 5.3: Orbital elements and trajectory for case C.

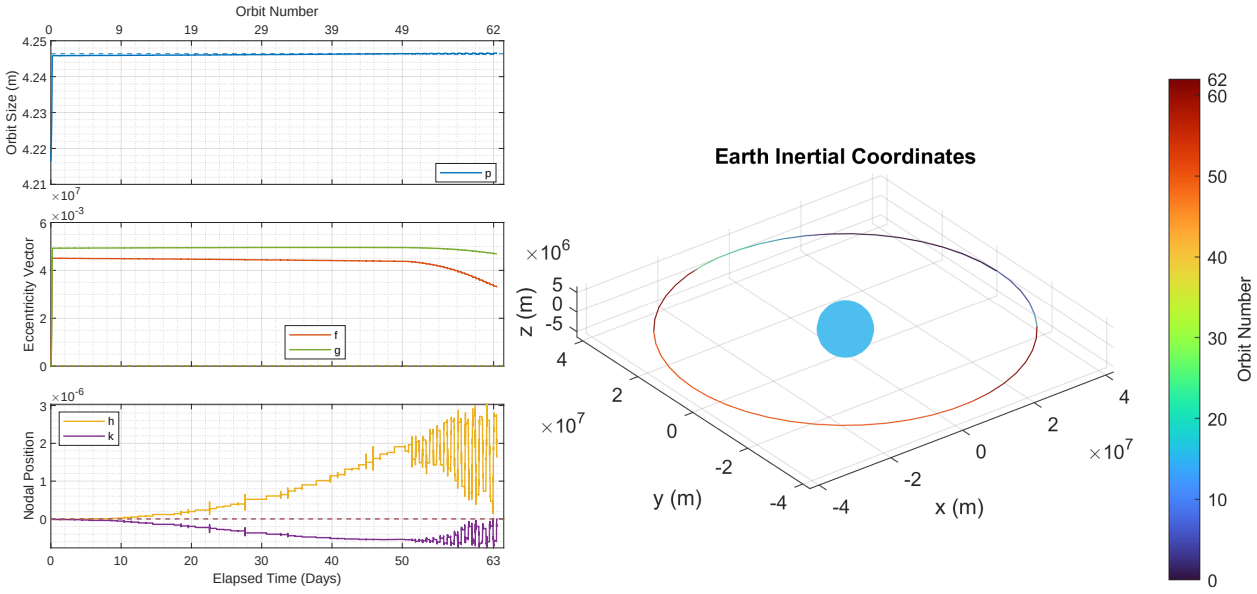

(a) Evolution of orbit elements in time. (b) Trajectory plot.

Figure 5.4: Orbital elements and trajectory for case D.

The "banding" of colours in the trajectory plots highlights the tendency of the guidance law to segment the trajectory into distinguishable phases rather than a smooth continuous maneuver. This can be attributed to the properties of the guidance law discussed in Section 3.6.1. Additionally, the tendency of the guidance law to continue changing orbital elements even after reaching their target values shows the relaxation of Lyapunov stability.

For case C, as speculated in the previous section, the guidance law does not smoothly vary the orbit. The direction of applied thrust varies by 180° thoughout the maneuver, and the Sun is not always in a suitable position for thrust production. Hence, even though the semilatus rectum (p) is supposed to remain constant, it varies so that some of the other orbital elements become easier to change. In effect, the guidance law has instated its own "intermediate orbit".

Case D highlights a significant issue with the guidance law: it is extremely slow to finish off "the last mile". Note that all of the cases were run with convergence tolerances exceeding 0.001 – this was done because smaller tolerances were either not achievable or took excessive numbers of orbits to converge.

This issue with last mile convergence may be attributed to the cone angle adaptation heuristic; not producing thrust exactly in the direction needed by the Q-Law incurs a sort of steady-state error similar to that in a proportional feedback controller.

5.1.2 Animations: Cases A-C

Animations of the trajectories in cases A-C are shown in the proceeding figures (case D is excluded because the change in shape is negligible). Seeing the trajectories animated in 3D space may help provide a more comprehensible view of what the guidance law is doing. Note that the 3D camera is rotated compared to the plots in the previous section.

Note: a JavaScript-enabled PDF viewer (e.g. Adobe Reader, Foxit Reader) is required for playing the animations.

Each animation plays at 10 frames per second by default, with approximately 50 frames of animation per case.

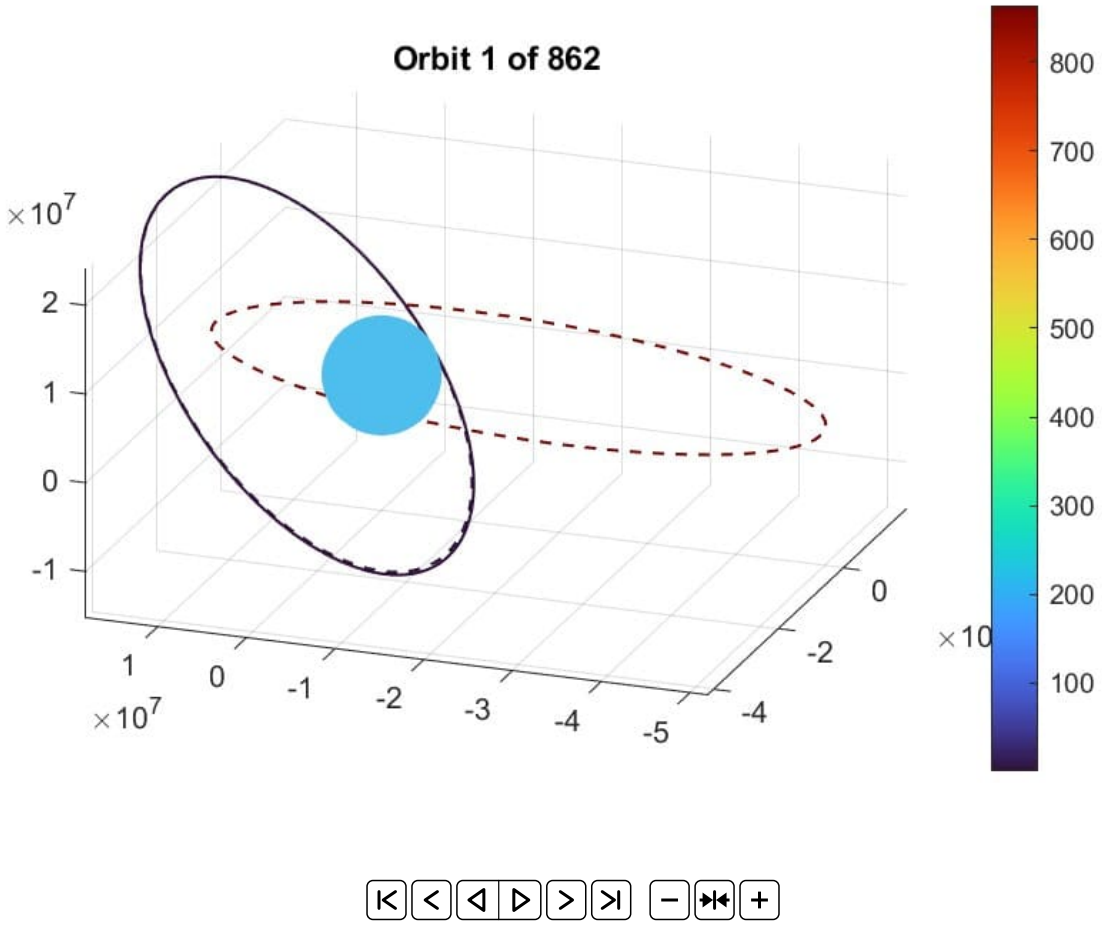

Figure 5.5: Trajectory animation for case A.

The segmentation of the trajectory is much easier to see in animation form. There are obvious points in the trajectory where the orbit "pauses", waiting for the Sun to move into a better position. This includes the time spent feathering the solar sail.

It is reasonable to conclude that time spent waiting for the Sun is essentially wasted, and there may exist a better trajectory that spends less time paused.

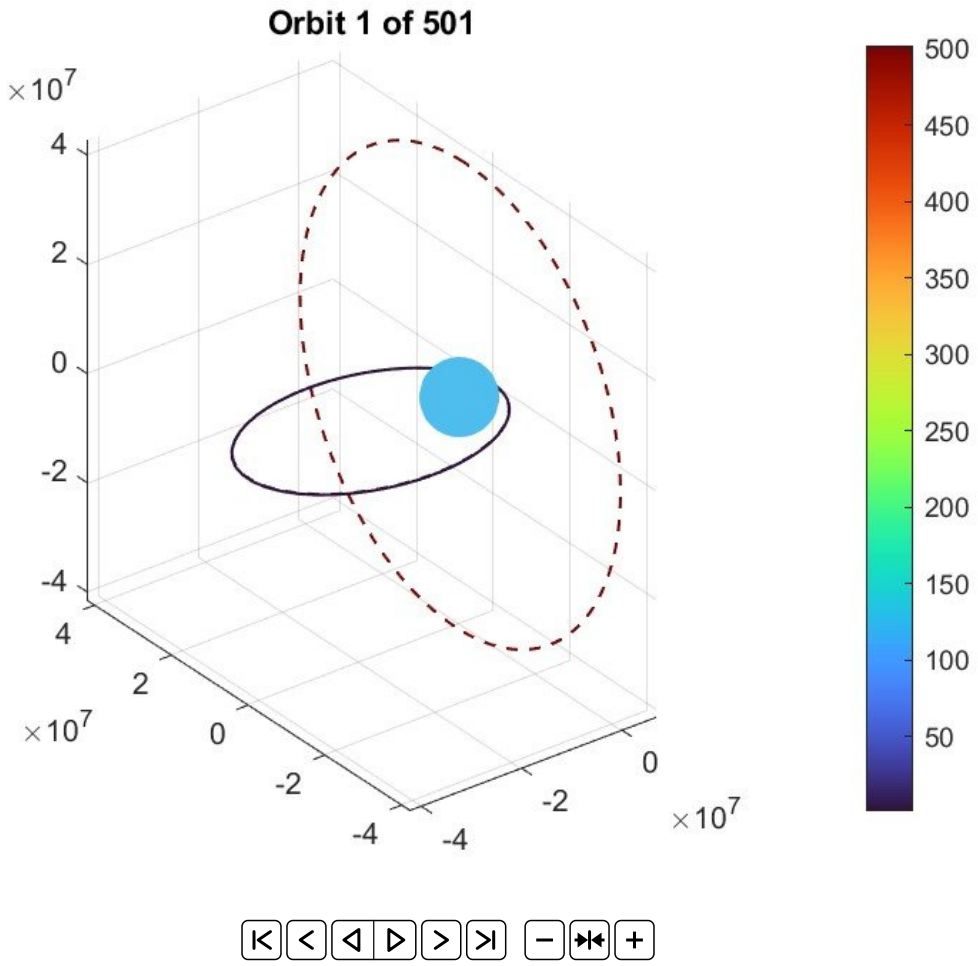

Figure 5.6: Trajectory animation for case B.

This trajectory is flown much more smoothly than in case A, but there is some stalling near the end.

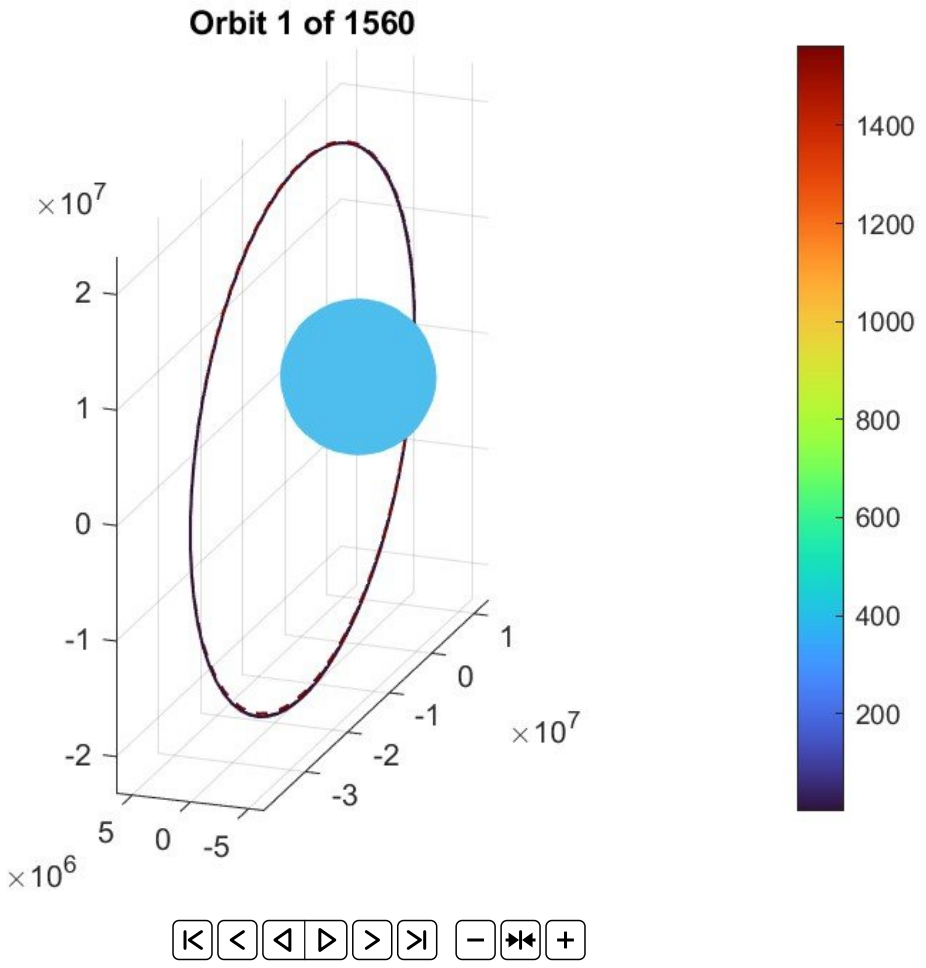

Figure 5.7: Trajectory animation for case C.

Trajectory segmentation is most evident in this animation.

Overall, it is impressive that the guidance law is convergent in all of the test cases. However, it is far from perfect. Most notably, it is extremely slow at advancing the orbit in certain segments. Hence, the first extended study aims to search for trajectories with a lower time of flight by tuning the guidance weights W_{oe}.

Tuning the weights of the Q-Law is equivalent to changing the "greediness strategy" of the local optimization being done at each timestep; the baseline Q-Law always attempts to maximize $-\dot{Q}$ (in a greedy fashion), and adjusting W_{oe} helps "steer the greediest direction" at one timestep to help the guidance law at a later timestep. There may exist a **local strategy** which can set up a better trajectory at a **global level**.

5.2 Time of Flight Optimization Study

Global weight optimization was performed for the first two baseline cases. The optimized guidance law tunings are compared against their unoptimized counterparts in Table 5.2.

Case	Time of Flight (d)	Number of Revolutions	Δv Expenditure (m/s)
A, Baseline	621	862	6459.6
A, Optimized	385	680	6216.1
B, Baseline	498	501	9640.5
B, Optimized	377	326	8315.4

Table 5.2: Comparison of optimized cases against their baselines.

The two cases still use their original convergence tolerances in the optimized tunings.

The improvement in time-of-flight (and number of revolutions) is remarkable. By inspecting the plots of the orbital elements in the proceeding section, it is clear that adjusting $W_{\text{œ}}$ changes the "strategy" employed by the guidance law.

One important note is that the stochastic optimization runs do not guarantee the discovery of a global minimum; the weights corresponding to the absolute lowest time of flight found across all optimization runs were used for the cases shown in the proceeding sections, but there may exist a solution with a lower time of flight that was not discovered. However, this is likely not a great issue; several different combinations of $W_{\text{œ}}$ all yielding a reduction in time of flight were found, and many solutions had a time of flight value within about 1% of the absolute minimum found in the optimization runs. It is highly unlikely then that a dramatically lower time of flight could have been found even with more compute time.

This highlights a great weakness of the approach taken by QUAIL – since there is so little that can be said about the guidance law analytically, it is very difficult to make any performance assertions about the global trajectory.

Another important point to make is that QUAIL requires fine-tuning to achieve a shorter time of flight. While it can work out of the box, it needs to be adjusted for each mission to fly trajectories more efficiently. This is much like how classical feedback control laws are tuned to match a certain control problem.

5.2.1 Plots

Baseline $W_{\text{œ}}$: $\{1, 1, 1, 1, 1\}$

Optimal $W_{\text{œ}}$: $\{1.774, 0.5149, 0.3327, 9.925, 0.5317\}$

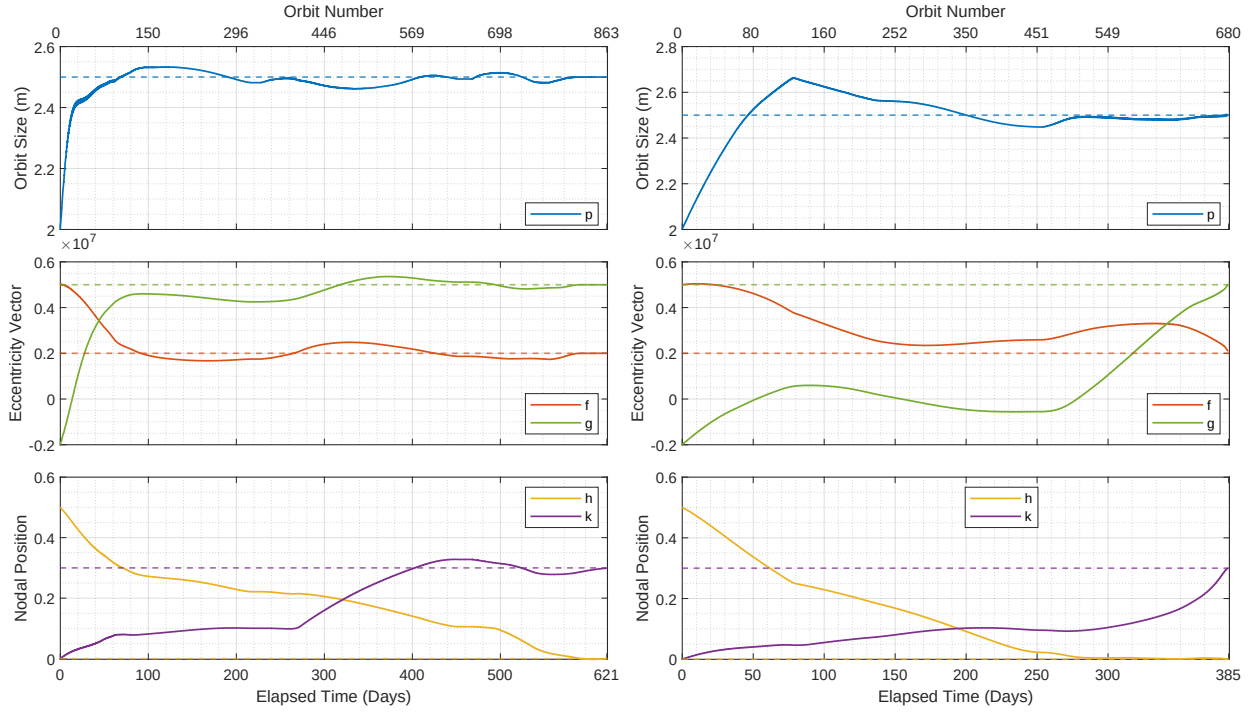

(a) Baseline. (b) Optimized.

Figure 5.8: Case A, orbital elements.

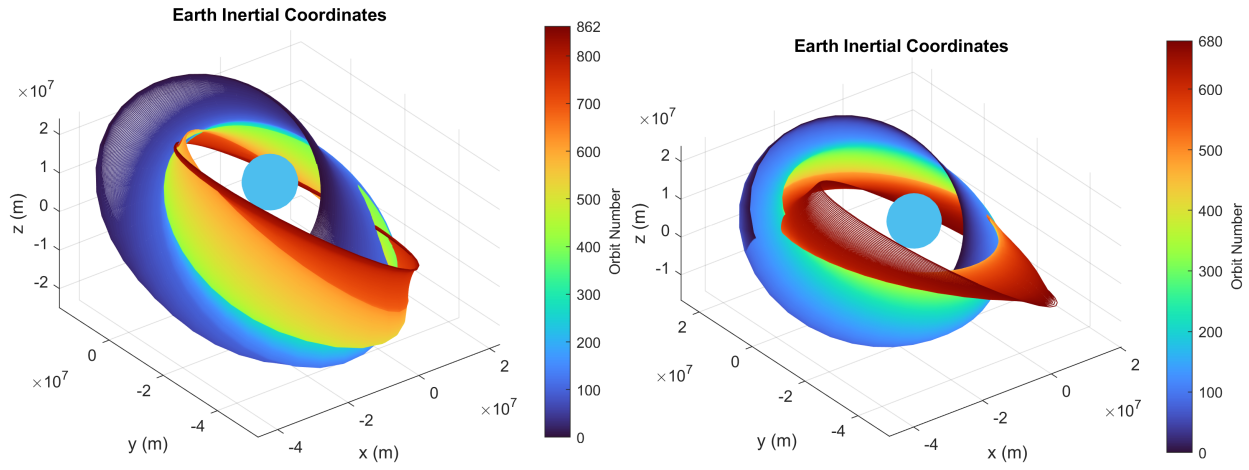

(a) Baseline. (b) Optimized.

Figure 5.9: Case A, trajectory plot.

5.2.2 Case B

Baseline $W_{\text{œ}}$: $\{1, 1, 1, 1, 1\}$

Optimal $W_{\text{œ}}$: $\{5.688, 1.178, 1.434, 3.545, 5.568\}$

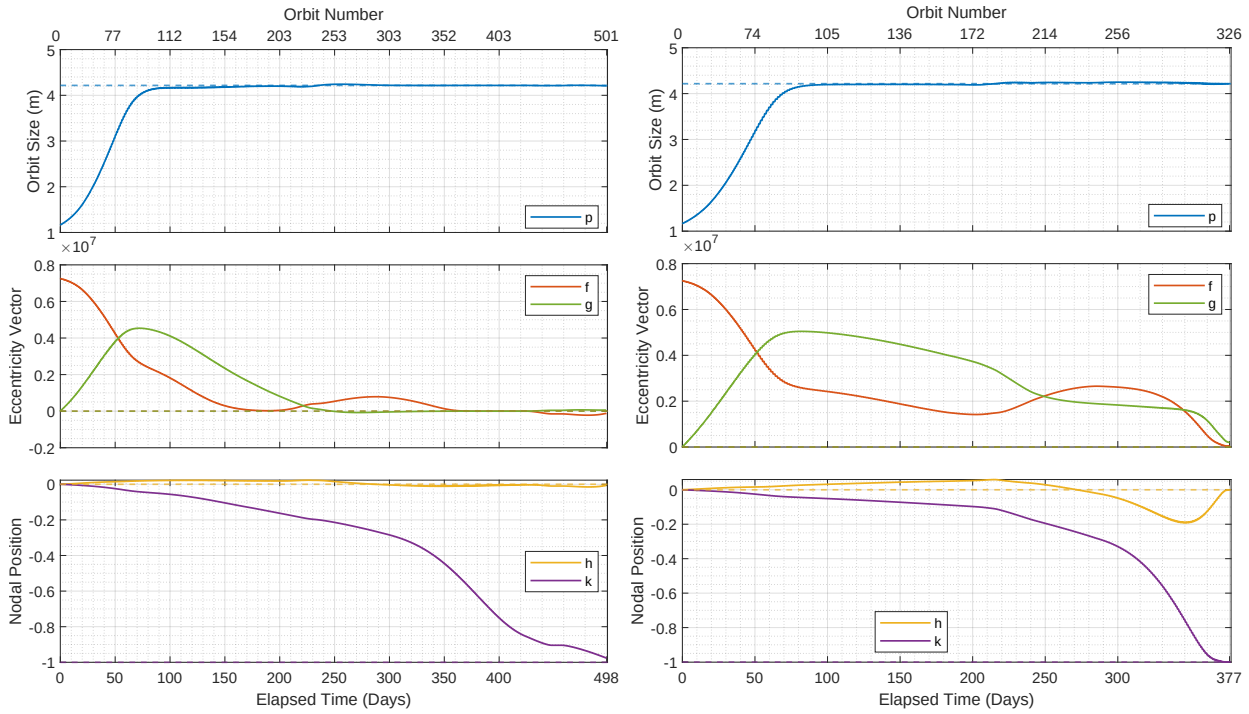

(a) Baseline. (b) Optimized.

Figure 5.10: Case B, orbital elements.

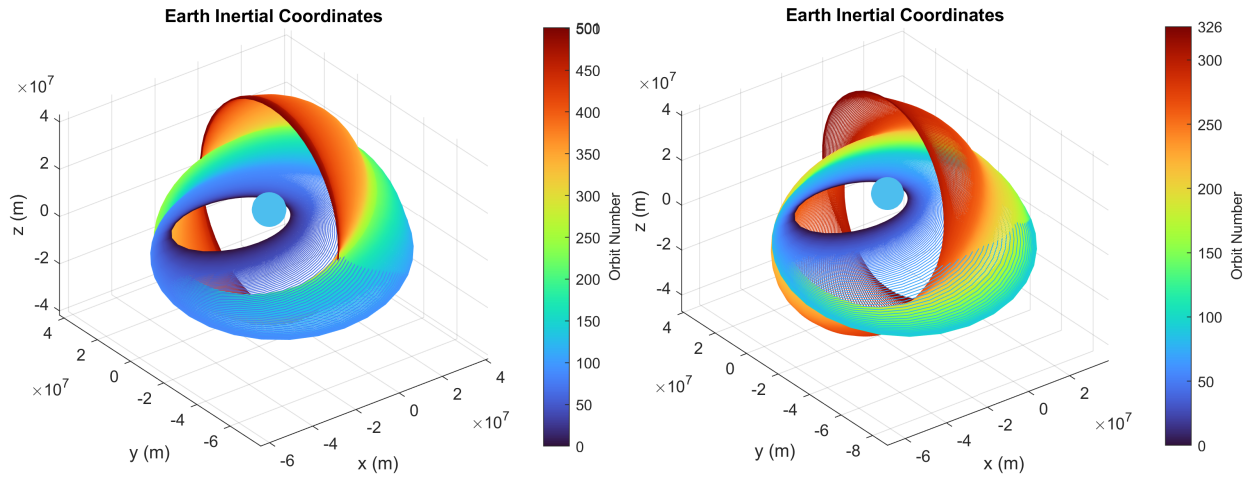

(a) Baseline. (b) Optimized.

Figure 5.11: Case B, trajectory plot.

5.2.3 Animations

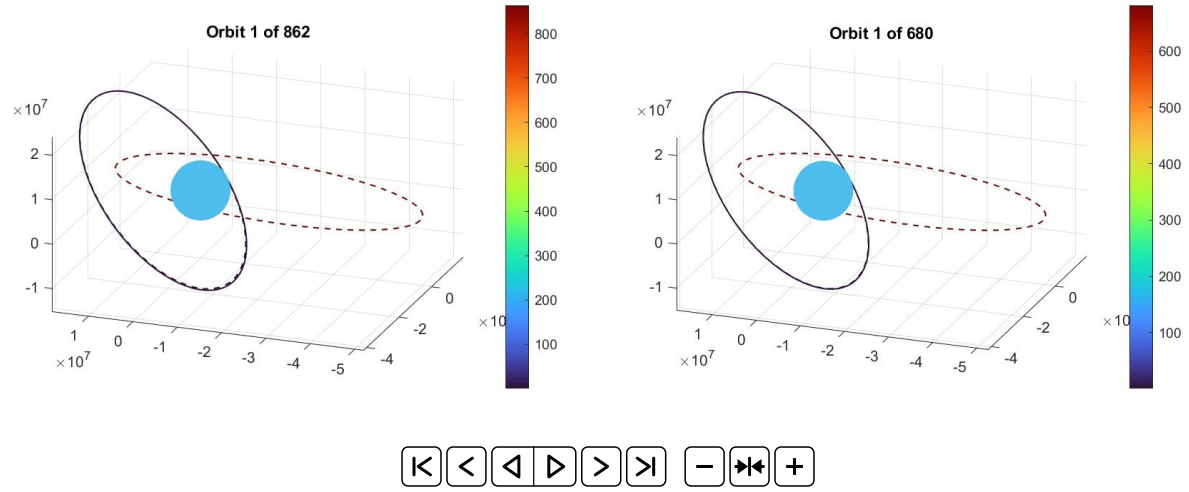

Figure 5.12: Case A before/after optimization.

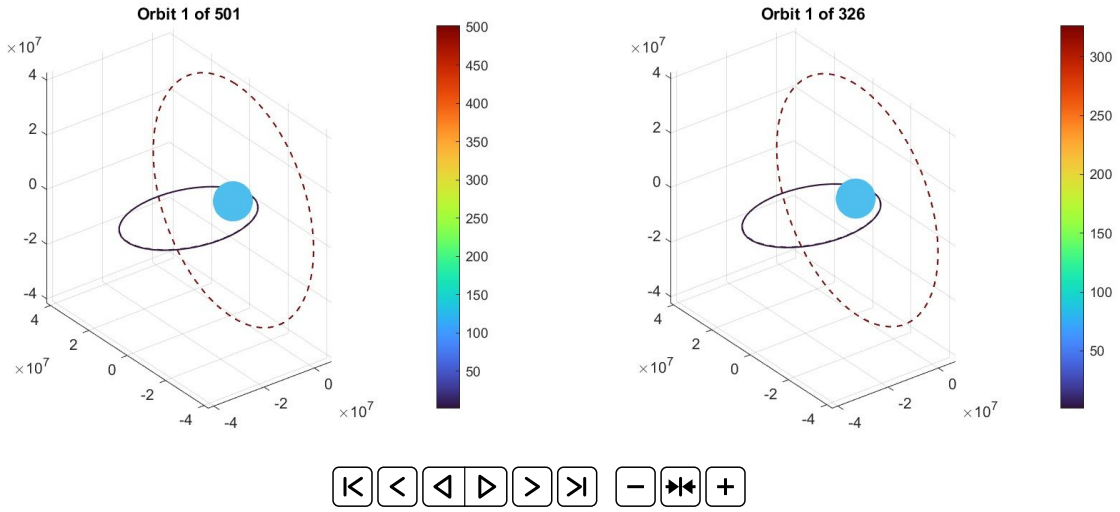

Figure 5.13: Case B before/after optimization.

By emphasizing certain elements over others, the guidance law is more willing to accept an increase in error in one element for a reduction in another. This allows the guidance law more wiggle room to disturb its trajectory to set up proceeding maneuvers.

The optimized transfers spend less time paused compared to their baseline counterparts. In Case A, the total Δv expenditures are very similar, but the trajectory taken by the optimized tuning looks far more direct than the baseline case. In Case B, Δv savings of 14% are achieved by taking a "shorter path".

The weights associated with each optimized case are not very obvious – it is not clear why emphasizing W_h in case A and W_p in case B result in much-improved performance. A possible mechanism for this happening is that $W_{\text{œ}}$ are tuned such that the local behaviour of the guidance law at each point in the trajectory "nicely sets up" the next part of the trajectory without any waiting needed.

5.3 Disturbance Rejection Study

The results of case J are shown below in Figure 5.14.

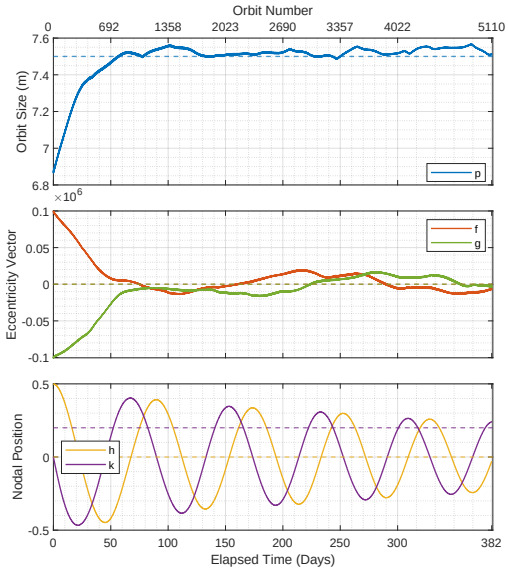

(a) Evolution of orbit elements in time.

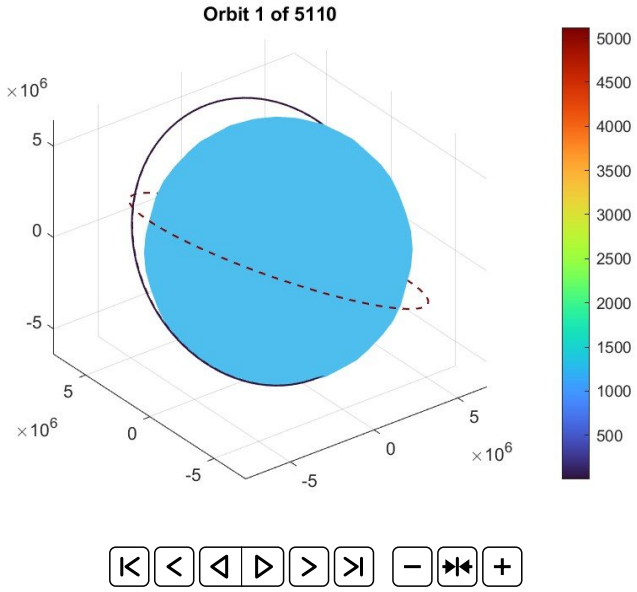

(b) Trajectory animation.

Figure 5.14: Orbital elements and trajectory for case J.

The effects of $J2$ perturbation are clearly visible in the plots of h and k. Despite the challenging conditions, QUAIL manages to perform the maneuver without issues.

It is interesting to note that the spacecraft performed over 5000 revolutions of Earth during its maneuver. This highlights the key advantage of using a feedback approach over a global method – a global optimization approach would likely be computationally intractable for a case like this.

5.4 Realistic Solar Sail Modelling Study

Cases A and B were run with modified values of κ, and with all other parameters kept the same as the baseline values. The impact on the time of flight is shown in Table 5.3.

	Time of Flight (d)	
κ	Case A	Case B
90°	1410	555
80°	1136	544
70°	941	515
60°	616	422
50°	1126	389
40°	1528	395
30°	2097	
20°		
10°		

Table 5.3: Variation of time of flight against an artificially restricted value of κ. Blank entries denote no convergence.

There is a clear optimum for κ, which is reasonable; that value represents the best tradeoff between producing thrust in the desired direction, and producing a sufficiently great amount of thrust.

Surprisingly, transfers are still working even with $\kappa = 40°$. This is a testament to the robustness of the Q-Law against plant dynamics variation, and suggests that QUAIL may work quite well even with very restrictive cone angle limits.

It is also reassuring to see that the guidance law has limits to its capabilities; for an extremely restrictive thrust cone angle, it simply cannot produce thrust in the direction needed by the Q-Law for progress toward the target orbit.

5.5 Discussion

While QUAIL demonstrates great success in all of the numerical experiments, the methodology must be scrutinized to assess the validity of the claims being made.

The lack of theoretical performance guarantees means that QUAIL can only be assessed through exhaustive simulation testing. In this thesis, only a handful of cases were simulated, and although they are challenging, they do not encompass the entire range of possible orbital maneuvers that may be done with a real solar sail. The issues encountered with the GEO disposal case raise concern over the performance of the guidance law with more "benign" orbital transfer cases, which may not have been captured by the other 3 cases. For future work, a better set of baseline cases should be developed, including a variety of cases motivated by practical maneuvers (de-orbiting, maneuvering to scientifically valuable orbits, etc.) rather than just trying to change many orbital elements all at once. **Both the quantity and quality of the trajectory cases should be improved** for future work. Nonetheless, the observed performance seen in the preceding experiments strongly suggests that QUAIL can perform complex orbital transfers.

The guidance optimization study is quite well done and shows that performance improvement is possible. However, no general trends or heuristics on how to tune the guidance law are developed, as there are only 2 cases that were optimized. An interesting study would be to develop a tuning heuristic for QUAIL which can be applied *a priori* or with fewer simulation runs, somewhat like Ziegler-Nichols PID tuning [39].

For disturbance rejection analysis, while $J2$ perturbations are dominant in low Earth orbit, most solar sails operate in higher orbits where these effects are not as significant. It would be more interesting to investigate gravitational perturbations from the Sun and Moon, or atmospheric drag effects. It is also difficult to justify claims about QUAIL's performance given that only a single case was run.

The realistic solar sail modelling study is quite limited in its scope and usefulness. An improved study with an actual thrust model featuring off-axis thrust may reveal more subtle features of working with solar sails that are not available with using an ideal sail thrust model.

Additionally, attitude dynamics have not been considered. For sufficiently long period orbits, this should not have a great effect on performance, but it would be desirable to test QUAIL in a simulator with limits imposed on the angular rates of the spacecraft.

Overall, the few experiments that were conducted with QUAIL cannot be used to certify performance, but suggest that even with further testing, QUAIL can prove to be a very reliable and performant guidance law for solar sailing.

Chapter 6

Significance and Future Work

An overview of the developed guidance law is presented, and potential areas for future work are identified.

6.1 Significance of QUAIL

QUAIL is a useful guidance law both for practical purposes, and also as an academically appealing demonstration of producing a guidance law for solar sails.

6.1.1 As a Product

A solar sailing guidance law for planetocentric maneuvering was developed, proving to be successful in a limited run of orbital transfer cases. This achievement in itself is significant, as there are very few examples of other guidance laws which can be used for this purpose.

The novel approach taken shows great promise for applicability to other areas. As shown in the extended studies, QUAIL can readily be modified and applied to different problems, making it excellent as both a mission planning tool and a design tool for developing new solar sail configurations. Since QUAIL does not explicitly depend on the thrust models of the solar sail, it can facilitate trajectory analysis for unique and esoteric spacecraft designs and will remain applicable as better reflection models for solar sails are developed.

The two main barriers holding back QUAIL from being dropped into a real spacecraft today are the lack of testing and the lack of consideration for solar sail attitude dynamics. However, further extension and development is highly likely to produce a workable solution.

6.1.2 As an Approach

The idea of ignoring solar sail dynamics in the Q-Law is highly unusual but produced amazingly good results with a very simple formulation. QUAIL is not elegant by any measure, but it is simple and effective. It is quite surprising that the approach of cascading a simple low-thrust guidance law with an additional stage for cone angle limits has not been attempted more widely.

This is very good news for the solar sail guidance community; being able to adapt the rich pool of research in conventional low-thrust guidance for solar sails means that significant progress could be made in the field by applying the approach taken for QUAIL to other low-thrust guidance laws. Bridging the gap between solar-sail-specific guidance research and the broader field of low-thrust guidance research can help the two communities work together to develop even better guidance laws in the future.

6.2 Future Work

An overview of the key directions for future work is discussed.

6.2.1 Outstanding Questions

The path forward for QUAIL can be summarized by the following questions:

- Can be formulation of QUAIL be adjusted to get better performance while still being relatively simple?
- How well will QUAIL work in simulations with a state-of-the-art solar sail thrust model?
- Can it be used around other planets/bodies? (e.g. Earth-Moon transfers)
- Can it target things other than Keplerian orbits? (e.g. Lagrange points, pole-sitting missions)
- Can the idea of cone angle limiting be applied to other solar sail problems, or even conventional low-thrust spacecraft?
- Can QUAIL solutions be used as a first guess for global optimization methods?

The main areas for improvement are then 1) Formulation 2) Dynamics and 3) Applications to New Problems.

6.2.2 Formulation Improvements

The formulation of QUAIL is simple and quite generic. Without adding too much additional complexity, some changes could be made to make it more performant.

Cone Angle Adaptation Heuristic Rework

The current approach for cone angle adaptation is simple and functional but lacks a solid mathematical justification for its design. Designing an adaptation scheme that is based on some form of mathematical optimality is desirable from a point of analysis, and may lead to better performance.

Coverstone [5] presents a feedback guidance law that maximizes the amount of thrust generated by a solar sail towards a given direction. Oguri [12] makes use of a similar approach. The idea is to find some $\hat{n} = \hat{n}^\dagger$ such that the product $\vec{F}(\hat{n}) \cdot \hat{n}^*$ (i.e. the projection of the resultant acceleration upon the ideal steering direction) is maximized. This can yield an orientation that is neither exactly on the surface of the thrust cone nor directly facing towards $\hat{n}^*$, but which maximizes the "amount of progress" made towards the ideal direction.

A further refinement to the above method could be made by restricting $\hat{n}$ to lie within the thrust cone. Given that the cone is a linear manifold, an analytical solution could be obtained similarly to Coverstone's formulation.

Higher Fidelity Q-Law Derivatives

The maximum rates of change for f and g are approximated in the Q-Law according to the formulation by Ref. [10]. However, Ref. [11] shows that a semi-analytical formulation can be readily obtained which gives an improved estimate.

6.2.3 Higher Fidelity Dynamics

The current dynamics model is very simple. Demonstration of robustness to plant model variation would be a very attractive attribute for the guidance law.

Solar Sail Thrust Models

So far, only a flat idealized sail has been used in simulations. Ref. [12] uses a more sophisticated thrust model incorporated into the Q-Law. It would be interesting to see how the guidance law produced in this project compares against Oguri's. A key advantage of QUAIL is that it can be applied to any solar sail thrust model without altering its formulation.

Testing QUAIL with a realistic thrust model may reveal issues in either the Q-Law or cone angle adaptation stage related to the fact that thrust is not produced directly towards the sail normal.

Incorporation of Attitude Dynamics

Attitude dynamics have been ignored for this project, but are essential for a guidance law to be usable. Adding an extra layer onto the simulator which accounts for attitude dynamics would be a simple way of testing QUAIL as-is.

A more interesting development would be to reformulate the second stage of the guidance law to consider not only the direction of the Sun, but also the agility of the solar sail. For example, there could be a second cone introduced, of width $\omega_{\max}\Delta t$ pointing in the direction $\hat{n}_{k-1}$, representing the attitude space that the solar sail can traverse in one timestep.

6.2.4 Applications to New Problems

This thesis is concerned only with geocentric orbits, but there is nothing stopping QUAIL from being applied to trajectories around other planets or even moons of planets.

Other Bodies

With increasing interest in cislunar space, it may be useful to investigate the applicability of solar sails for translunar trajectories.

There are also missions using solar sails to the inner solar system, such as a Mercury sample return mission proposed by Hughes [40]. Although the guidance law developed in this project is targeted at planetocentric orbits, it may also work for heliocentric trajectories.

Non-Keplerian Orbits

Solar sails are a prime candidate for exploiting non-Keplerian trajectories such as halo orbits around Lagrange points; the lack of propellant consumption leads to an uncapped mission life in a frozen orbit. Applying the guidance law to a multi-body problem could give interesting results, but is made difficult by the lack of orbital elements to describe such trajectories.

As a Starting Point for Global Methods

Many Q-Law papers describe the possibility of using solutions obtained by their guidance law to initialize a global method, *but no one appears to have actually done so*. The trajectories

produced by QUAIL could be used as an initial guess for global methods to kickstart their optimization processes. This would address two important research gaps:

1. Using Lyapunov methods (i.e. Q-Laws) to generate initial guesses for high-fidelity trajectory optimization is a frequently mentioned but unexplored direction.

2. Generating good initial guesses for global optimization of solar sail trajectories is difficult.

A Q-Law (either QUAIL, its predecessors, or a derivative) could be used in conjunction with a simulator to integrate an initial trajectory forward in time to reach a final target orbit. The position history flown by the Q-Law can then be used as the starting point for a pseudospectral global trajectory optimization scheme. Q-Law solutions are cheap to evaluate because the cost is about as much as propagating an orbit in time. Using such a solution to initialize a global optimization run will save expensive iterations, and could result in better convergence characteristics.

6.3 Life Lessons from a Guidance Law

To close off this thesis, the 5 most important points discussed in solving the planetocentric guidance problem for solar sails are listed below, along with an accompanying life lesson.

1. Use feedback guidance instead of solving for a global trajectory.
   Take things one step at a time.

2. Assume a solar-sail-agnostic thrust model for the Q-Law.
   Keep it simple.

3. Adapt the solution from the Q-Law to make it work for solar sails.
   Be willing to try something unconventional.

4. Relax Lyapunov stability.
   Sometimes it must get worse before it gets better.

5. Adjust the strategy of the guidance law to set up future maneuvers in a favourable position.
   Set up others for success.

References

[1] Dan Lev, Roger M Myers, Kristina M Lemmer, Jonathan Kolbeck, Hiroyuki Koizumi, and Kurt Polzin, "The Technological and Commercial Expansion of Electric Propulsion," *Acta Astronautica*, Vol. 159, pp. 213–227, 2019.

[2] David A Spencer, Bruce Betts, John M Bellardo, Alex Diaz, Barbara Plante, and Justin R Mansell, "The Lightsail 2 Solar Sailing Technology Demonstration," *Advances in Space Research*, Vol. 67, No. 9, pp. 2878–2889, 2021.

[3] Osamu Mori, Hirotaka Sawada, Ryu Funase, Mutsuko Morimoto, Tatsuya Endo, Takayuki Yamamoto, Yuichi Tsuda, Yasuhiro Kawakatsu, Jun'ichiro Kawaguchi, Yasuyuki Miyazaki, *et al.*, "First Solar Power Sail Demonstration by IKAROS," *Transactions of the Japan Society for Aeronautical and Space Sciences, Aerospace Technology Japan*, Vol. 8, No. ists27, pp. 425–431, 2010.

[4] Paul D Fieseler, "A Method for Solar Sailing in a Low Earth Orbit," *Acta Astronautica*, Vol. 43, No. 9-10, pp. 531–541, 1998.

[5] Victoria L Coverstone and John E Prussing, "Technique for Escape from Geosynchronous Transfer Orbit Using a Solar Sail," *Journal of Guidance, Control, and Dynamics*, Vol. 26, No. 4, pp. 628–634, 2003.

[6] V Lappas, S Pellegrino, H Guenat, M Straubel, H Steyn, V Kostopoulos, E Sarris, O Takinalp, S Wokes, and A Bonnema, "DEORBITSAIL: De-orbiting of Satellites Using Solar Sails," in *2011 2nd International Conference on Space Technology*, IEEE, 2011, pp. 1–3.

[7] Colin R McInnes, *Solar Sailing: Technology, Dynamics and Mission Applications*. Springer Science & Business Media, 2004.

[8] Marc R Ilgen, "Low Thrust OTV Guidance Using Liapunov Optimal Feedback Control Techniques," *Astrodynamics 1993*, pp. 1527–1545, 1994.

[9] Anastassios Petropoulos, "Low-thrust Orbit Transfers Using Candidate Lyapunov Functions with a Mechanism for Coasting," in *AIAA/AAS Astrodynamics Specialist Conference and Exhibit*, 2004, p. 5089.

[10] Gábor Varga and José Manuel Sánchez Pérez, "Many-revolution Low-thrust Orbit Transfer Computation Using Equinoctial Q-Law Including J2 and Eclipse Effects," *Advances in the Astronautical Sciences*, Vol. 156, pp. 2463–2481, 2016.

[11] Sanjeev Narayanaswamy and Christopher J. Damaren, "Equinoctial Lyapunov Control Law for Low-thrust Rendezvous," en, *Journal of Guidance, Control, and Dynamics*, Vol. 46, No. 4, pp. 781–795, Apr. 2023.

[12] Kenshiro Oguri, Gregory Lantoine, Anastassios E Petropoulos, and Jay W McMahon, "Solar Sailing Q-law for Planetocentric, Many-revolution Sail Orbit Transfers," *Journal of Guidance, Control, and Dynamics*, pp. 1–10, 2023.

[13] CH Yam, DD Lorenzo, and D Izzo, "Low-thrust Trajectory Design as a Constrained Global Optimization Problem," *Proceedings of the Institution of Mechanical Engineers, Part G: Journal of Aerospace Engineering*, Vol. 225, No. 11, pp. 1243–1251, 2011.

[14] Christopher Damaren, Anton H. J. De Ruiter, and James R Forbes, *Spacecraft Dynamics and Control: An Introduction*, 1st ed. Wiley, 2013.

[15] Michael JH Walker, B Ireland, and Joyce Owens, "A Set of Modified Equinoctial Orbit Elements," *Celestial mechanics*, Vol. 36, No. 4, pp. 409–419, 1985.

[16] Gooding Universal Elements, 2021.

[17] David Morante, Manuel Sanjurjo Rivo, and Manuel Soler, "A Survey on Low-thrust Trajectory Optimization Approaches," *Aerospace*, Vol. 8, No. 3, p. 88, 2021.

[18] Matthew P Kelly, "Transcription Methods for Trajectory Optimization," *Tutorial, Cornell University, Feb*, p. 21, 2015.

[19] Jon A Sims and Steve N Flanagan, "Preliminary Design of Low-thrust Interplanetary Missions," 1997.

[20] Fariba Fahroo and I Michael Ross, "Direct Trajectory Optimization by a Chebyshev Pseudospectral Method," *Journal of Guidance, Control, and Dynamics*, Vol. 25, No. 1, pp. 160–166, 2002.

[21] Sanjeev Narayanaswamy and Christopher J Damaren, "Comparison of the Legendre–Gauss Pseudospectral and Hermite–Legendre–Gauss–Lobatto Methods for Low-thrust Spacecraft Trajectory Optimization," *Aerospace Systems*, Vol. 3, No. 1, pp. 53–70, 2020.

[22] Bo James Naasz, "Classical Element Feedback Control for Spacecraft Orbital Maneuvers," Ph.D. Dissertation, Virginia Tech, 2002.

[23] Mirue Choi and Christopher J Damaren, "Structural Dynamics and Attitude Control of a Solar Sail Using Tip Vanes," *Journal of Spacecraft and Rockets*, Vol. 52, No. 6, pp. 1665–1679, 2015.

[24] Elena Polyakhova and Vladimir Korolev, "The Solar Sail: Current State of the Problem," in *AIP Conference Proceedings*, Vol. 1959, 1, AIP Publishing, 2018.

[25] Hiraku Sakamoto, KC Park, and Yasuyuki Miyazaki, "Effect of Static and Dynamic Solar Sail Deformation on Center of Pressure and Thrust Forces," in *AIAA Guidance, Navigation, and Control Conference and Exhibit*, 2006, p. 6184.

[26] Leonard Felicetti, Matteo Ceriotti, and Patrick Harkness, "Attitude Stability and Altitude Control of a Variable-geometry Earth-orbiting Solar Sail," *Journal of Guidance, Control, and Dynamics*, Vol. 39, No. 9, pp. 2112–2126, 2016.

[27] Yuichi Tsuda, Osamu Mori, Ryu Funase, Hirotaka Sawada, Takayuki Yamamoto, Takanao Saiki, Tatsuya Endo, Katsuhide Yonekura, Hirokazu Hoshino, and Jun'ichiro Kawaguchi, "Achievement of Ikaros—japanese Deep Space Solar Sail Demonstration Mission," *Acta Astronautica*, Vol. 82, No. 2, pp. 183–188, 2013.

[28] Les Johnson, Roy Young, Edward Montgomery, and Dean Alhorn, "Status of Solar Sail Technology Within NASA," *Advances in Space Research*, Vol. 48, No. 11, pp. 1687–1694, 2011.

[29] Leonel Rios-Reyes and Daniel J Scheeres, "Generalized Model for Solar Sails," *Journal of Spacecraft and Rockets*, Vol. 42, No. 1, pp. 182–185, 2005.

[30] Yuichi Tsuda, Takanao Saiki, Ryu Funase, and Yuya Mimasu, "Generalized Attitude Model for Spinning Solar Sail Spacecraft," *Journal of Guidance, Control, and Dynamics*, Vol. 36, No. 4, pp. 967–974, 2013.

[31] Lester L Sackett, "Optimal Solar Sail Planetocentric Trajectories," 1977.

[32] Malcolm Macdonald and Colin R McInnes, "Analytical Control Laws for Planet-centered Solar Sailing," *Journal of Guidance, Control, and Dynamics*, Vol. 28, No. 5, pp. 1038–1048, 2005.

[33] HD Curtis, Orbital Mechanics for Students, 2014.

[34] James H Verner, "Numerically Optimal Runge–kutta Pairs with Interpolants," *Numerical Algorithms*, Vol. 53, No. 2-3, pp. 383–396, 2010.

[35] Pauli Virtanen, Ralf Gommers, Travis E. Oliphant, Matt Haberland, Tyler Reddy, David Cournapeau, Evgeni Burovski, Pearu Peterson, Warren Weckesser, Jonathan Bright, Stéfan J. van der Walt, Matthew Brett, Joshua Wilson, K. Jarrod Millman, Nikolay Mayorov, Andrew R. J. Nelson, Eric Jones, Robert Kern, Eric Larson, C J Carey, İlhan Polat, Yu Feng, Eric W. Moore, Jake VanderPlas, Denis Laxalde, Josef Perktold, Robert Cimrman, Ian Henriksen, E. A. Quintero, Charles R. Harris, Anne M. Archibald, Antônio H. Ribeiro, Fabian Pedregosa, Paul van Mulbregt, and SciPy 1.0 Contributors, "SciPy 1.0: Fundamental Algorithms for Scientific Computing in Python," *Nature Methods*, Vol. 17, pp. 261–272, 2020.

[36] Hao Mei, Christopher J Damaren, and Xingqun Zhan, "Hybrid removal of end-of-life geosynchronous satellites using solar radiation pressure and impulsive thrusts," *Advances in Space Research*, Vol. 66, No. 4, pp. 974–991, 2020.

[37] Richard P Brent, *Algorithms for Minimization Without Derivatives*. Courier Corporation, 2013.

[38] NASA Service Preparation Subsystem (SPS) and Mission Planning Group (MPG), Modified Equinoctial Orbital Elements, 2006.

[39] John G Ziegler and Nathaniel B Nichols, "Optimum settings for automatic controllers," *Transactions of the American society of mechanical engineers*, Vol. 64, No. 8, pp. 759–765, 1942.

[40] Gareth W Hughes, Malcolm Macdonald, Colin R McInnes, Alessandro Atzei, and Peter Falkner, "Sample Return from Mercury and Other Terrestrial Planets Using Solar Sail Propulsion," *Journal of spacecraft and rockets*, Vol. 43, No. 4, pp. 828–835, 2006.